

Supplementary Information for

Two appealing alternatives for MOFs synthesis: solvent-free oven heating vs microwave heating

Mónica Lanchas,^a Sandra Arcediano,^a Andrés T. Aguayo,^b Garikoitz Beobide,^{*a} Oscar Castillo,^{*a}
Javier Cepeda,^a Daniel Vallejo-Sánchez^a and Antonio Luque^a

^a *Departamento de Química Inorgánica, Facultad de Ciencia y Tecnología, Universidad del País Vasco, UPV/EHU, Apartado 644, E-48080 Bilbao, Spain and* ^b *Departamento de Ingeniería Química, Facultad de Ciencia y Tecnología, UPV/EHU, Universidad del País Vasco, Apartado 644, E-48080 Bilbao, Spain.*

S1. SOLVENT-FREE SYNTHESIS BY OVEN HEATING AND MICROWAVE IRRADIATION	2
S2. THERMOGRAVIMETRIC ANALYSIS AND FTIR SPECTRA	10
S3. X-RAY POWDER DIFFRACTION ANALYSIS	16
S4. EFFECT OF THE HEATING RATES AND SOURCE ON SAMPLE CRYSTALLINITY	21
S5. N₂ ADSORPTION EXPERIMENTS	32
S6. COMPARATIVE BETWEEN SYNTHESIS ROUTE AND SURFACE AREA	41

S1. SOLVENT-FREE SYNTHESIS BY OVEN HEATING AND MICROWAVE IRRADIATION

Chemicals

All the chemicals were of reagent grade and were used as commercially obtained.

Synthesis

Samples were prepared according to the following general procedure. The corresponding amounts of the metal source ($\text{Co}(\text{OH})_2$, $\text{Cu}(\text{acetate})_2 \cdot \text{H}_2\text{O}$, $\text{FeCl}_3 \cdot 6\text{H}_2\text{O}$, $\text{Fe}(\text{NO}_3)_3 \cdot 9\text{H}_2\text{O}$) and the bridging ligand (2-methylimidazole (mIm) or benzene-1,3,5-tricarboxylic acid (BTC)) were hand-grinded thoroughly to obtain a homogeneous mixture. In the case of the solvent-free synthesis by oven-heating, the final reagent mixture was introduced into a glass ampoule and heated with the thermal processes described in Table S1.1. The glass ampoule was sealed in all cases except for the synthesis of MIL-100(Fe/Cl). Table S1.2 and S1.4 shows the details on the preparation of each sample. Details on the samples prepared by microwave assisted solvent-free synthesis are gathered on Table S1.3 and S.1.5. As microwave source the following conventional household microwave oven was used. In the case of microwave heating, the energy consumption was about 30 and 300 J per gram of product.



All the products were washed with ethanol to remove unreacted and sequentially characterized by FTIR spectroscopy, thermogravimetric analysis (TGA) and X-ray powder diffraction (XRPD). The reaction yields are based on the metal and, except for ZIF-67, they were calculated from the weight of the dry product (desolvated). As ZIF-67 samples present a minor amount of unreacted and insoluble $\text{Co}(\text{OH})_2$, its reaction yields were calculated from the thermogravimetric data, on the

basis of the weight of the final residue and the weight of the metal imidazolate once it has lost all guest molecules.

The identification of the MOF crystal structure was made scrutinizing the Cambridge Structural Database on the basis of the experimental XRPD data of the synthesized samples (for further details see section S3). Effect of the heating rate and microwave irradiation conditions in the crystallinity and microstructural features of synthesized products are discussed in section S4, while details concerning N₂ adsorption experiments and surface area determinations are gathered in section S5.

Physical Measurements

The purity and homogeneity of the polycrystalline samples were checked by elemental analysis, IR spectroscopy, thermogravimetric measurements and X-ray powder diffraction methods. Elemental analyses (C, H, N) were performed on a Euro EA Elemental Analyzer, whereas the metal content determined by a Horiba Yobin Yvon Activa inductively coupled plasma atomic emission spectrometer (ICP-AES). The IR spectra (KBr pellets) were recorded on a FTIR 8400S Shimadzu spectrometer in the 4000–400 cm⁻¹ spectral region. Thermal analyses (TG/DTA) were performed on a TA Instruments SDT 2960 thermal analyzer in a synthetic air atmosphere (79% N₂ / 21% O₂) with a heating rate of 5°C min⁻¹. The permanent porosity of all samples was studied by means of the measurements of N₂ adsorption isotherms at 77 K using a *Micromeritics* ASAP 2010 analyser. Samples were dried under vacuum at 140 °C and *ca.* 1·10⁻⁴ atm during 6 h prior to measurements.

Table S1.1. Employed thermal programs.

Code	Thermal program	Code	Thermal program
1	<p>160°C 100°C RT 30°C 2 h 6 h 12h</p>	4	<p>120°C RT 30°C 48 h s/t</p>
2	<p>160°C 100°C RT 30°C 2 h 48 h 12h</p>	5	<p>140°C RT 30°C 28 h s/t</p>
3	<p>120°C RT 30°C 24 h s/t</p>	6	<p>160°C RT 30°C 144 h 12h</p>

Table S1.2. Oven-heated solvent-free synthesis: synthesis conditions, sample code and formulae of the synthesised MOF, yield and corresponding CSD (Cambridge Structural Database) code.¹

M:L	Synthesis ratio	Reactants	Thermal program	Sample code	MOF and Formulae	Yield (%)	CSD
Co:mIm	1:2.1	<i>Co(OH)</i> ₂ : 4 mmol (0.3914 g) <i>mIm</i> : 8.4 mmol (0.6966 g)	1	ZIF67-OH1	ZIF-67	89.4	GITTOT01
			2	ZIF67-OH2	[Co(mIm) ₂] _n	91.7	
Cu:BTC	3:2	<i>Cu(acetate)</i> ₂ : 3 mmol (0.6050 g) <i>BTC</i> : 2 mmol (0.4424 g)	3	MOF199-OH1	MOF-199	89.0	UVIPIZ
			4	MOF199-OH2	[Cu ₃ (μ ₆ -BTC) ₂ (OH ₂) ₃] _n	99.3	
Fe:BTC	3:2	<i>FeCl</i> ₃ : 3 mmol (0.8110 g) <i>BTC</i> : 2 mmol (0.4424 g)	3	MIL-C-OH1	MIL-100(Fe/Cl)	40.3	CIGXIA ²
			4	MIL-C-OH2		34.4	
			5	MIL-C-OH3	48.4		
			7	MIL-C-OH4	[Fe ₃ (μ ₃ -O)(μ ₆ -BTC) ₂ Cl(OH ₂) ₂] _n	78.9	
			8	MIL-C-OH6	66.3		
Fe:BTC	3:2	<i>Fe(NO₃)₃</i> : 3 mmol (1.2367 g) <i>BTC</i> : 2 mmol (0.4424 g)	3	MIL-N-OH1	MIL-100(Fe/NO ₃)	42.0	CIGXIA ²
			4	MIL-N-OH2		52.2	
			5	MIL-N-OH3	91.4		
			7	MIL-N-OH4	[Fe ₃ (μ ₃ -O)(μ ₆ -BTC) ₂ (NO ₃)(OH ₂) ₂] _n	82.0	
			8	MIL-N-OH6	75.1		
Co:Propionic acid:Adenine	1:3.4:1	<i>Co(OH)</i> ₂ : 8 mmol (0.7827 g) <i>Propionic acid</i> : 27 mmol (2.0 mL) <i>Adenine</i> : 8 mmo (1.092 g)	6	MBioF-OH1	MBioF-12 [Co(μ-propionate)(μ ₃ -adeninate)] _n	90.1	BEYSEF

¹: *mIm*: 2-methylimidazole; *BTC*: *benzene-1,3,5-tricarboxylic acid*.

² CIGXIA: it corresponds to MIL-100(Fe/F) with formula [Fe₃(μ₃-O)(μ₆-BTC)₂F(OH₂)₂]_n.

Table S1.3. Microwave assisted solvent-free synthesis: synthesis conditions, sample code and formulae of the synthesised MOF, yield and corresponding CSD (Cambridge Structural Database) code.¹

M:L	Synthesis ratio	Reactants	Microwave irradiation	Sample code	MOF and Formulae	Yield (%)	CSD
Co:mIm	1:2.1	<i>Co(OH)₂</i> : 4 mmol (0.3914 g) <i>mIm</i> : 8.4 mmol (0.6966 g)	6 min, 100%	ZIF67-MW1	ZIF-67 [Co(mIm) ₂] _n	89.8	GITTOT01
			7.5 min, 80%	ZIF67-MW2		91.3	
			12 min, 50%	ZIF67-MW3		88.3	
			20 min, 30%	ZIF67-MW4		89.6	
Cu:BTC	3:2	<i>Cu(acetate)₂</i> : 3 mmol (0.6050 g) <i>BTC</i> : 2 mmol (0.4424 g)	6 min, 100%	MOF199-MW1	MOF-199 [Cu ₃ (μ ₆ -BTC) ₂ (OH ₂) ₃] _n	97.1	UUIPIZ
			7.5 min, 80%	MOF199-MW2		88.8	
			12 min, 50%	MOF199-MW3		96.8	
			20 min, 30%	MOF199-MW4		97.3	
Fe:BTC	3:2	<i>FeCl₃</i> : 3 mmol (0.8110 g) <i>BTC</i> : 2 mmol (0.4424 g)	0.8 min, 100%	MIL-C-MW1	MIL-100(Fe/Cl) [Fe ₃ (μ ₃ -O)(μ ₆ -BTC) ₂ Cl(OH ₂) ₂] _n	23.5	CIGXIA ²
			1.0 min, 80%	MIL-C-MW2		17.2	
			1.6 min, 50%	MIL-C-MW3		40.7	
			2.7 min, 30%	MIL-C-MW4		25.9	
			3 min, 50%	MIL-C-MW5		80.1	
			4 min, 30%	MIL-C-MW6		77.2	
Fe:BTC	3:2	<i>Fe(NO₃)₃</i> : 3 mmol (1.2367 g) <i>BTC</i> : 2 mmol (0.4424 g)	0.8 min, 100%	MIL-N-MW1	MIL-100(Fe/NO ₃) [Fe ₃ (μ ₃ -O)(μ ₆ -BTC) ₂ (NO ₃)(OH ₂) ₂] _n	57.2	CIGXIA ²
			1.0 min, 80%	MIL-N-MW2		31.4	
			1.6 min, 50%	MIL-N-MW3		51.8	
			2.7 min, 30%	MIL-N-MW4		71.0	
			3 min, 50%	MIL-N-MW5		82.2	
			4 min, 30%	MIL-N-MW6		82.9	
Co:Propionic acid:Adenine¹	1:3.4:1	<i>Co(OH)₂</i> : 8 mmol (0.7827 g) <i>Propionic acid</i> : 27 mmol (2.0 mL) <i>Adenine</i> : 8 mmol (1.092 g)	6 min, 100%	MBioF-MW1	MBioF-12 [Co(μ-propionate)(μ ₃ -adeninate)] _n	89.8	BEYSEF
			7.5 min, 80%	MBioF -MW2		91.3	
			12 min, 50%	MBioF -MW3		88.3	
			20 min, 30%	MBioF -MW4		89.6	

¹ The excess of propionic acid accounts for the propionic acid that goes to the gas-phase.

Table S1.4. Oven heating solvent-free synthesis of MIL-N-OH and MIL-C-OH with an stoichiometric amount of NaOH: synthesis conditions, sample code and formulae of the synthesised MOF, yield and corresponding CSD (Cambridge Structural Database) code.¹

M:L	Synthesis ratio	Reactants	Thermal program	Sample code	MOF and Formulae	Yield (%)	CSD
Fe:BTC	3:2:3	<i>FeCl</i> ₃ : 3 mmol (0.8110 g) <i>BTC</i> : 2 mmol (0.4424 g) <i>NaOH</i> : 3 mmol (0.1237 g)	7	MIL-C-OH5	MIL-100(Fe/Cl) [Fe ₃ (μ ₃ -O)(μ ₆ -BTC) ₂ Cl(OH ₂) ₂] _n	62.2	CIGXIA ²
Fe:BTC	3:2:3	<i>Fe(NO</i> ₃) ₃ : 3 mmol (1.2367 g) <i>BTC</i> : 2 mmol (0.4424 g) <i>NaOH</i> : 3 mmol (0.1237 g)	7	MIL-C-OH5	MIL-100(Fe/NO ₃) [Fe ₃ (μ ₃ -O)(μ ₆ -BTC) ₂ (NO ₃)(OH ₂) ₂] _n	99.1	CIGXIA ²

Table S1.5. Microwave assisted solvent-free synthesis of MIL-N-MW with an stoichiometric amount of NaOH: synthesis conditions, sample code and formulae of the synthesised MOF, yield and corresponding CSD (Cambridge Structural Database) code.¹

M:L:NaOH	Synthesis ratio	Reactants	Microwave irradiation	Sample code	MOF and Formulae	Yield (%)	CSD
			0.8 min, 100%	MIL-N-MW1'		60.0	
Fe:BTC:NaOH	3:2:3	<i>Fe(NO₃)₃</i> : 3 mmol (1.2367 g) <i>BTC</i> : 2 mmol (0.4424 g) <i>NaOH</i> : 3 mmol (0.1237 g)	1.0 min, 80%	MIL-N-MW2'	MIL-100(Fe/NO ₃)	54.3	CIGXIA ²
			1.6 min, 50%	MIL-N-MW3'	[Fe ₃ (μ ₃ -O)(μ ₆ -BTC) ₂ (NO ₃)(OH ₂) ₂] _n	50.3	
			2.7 min, 30%	MIL-N-MW4'		78.4	

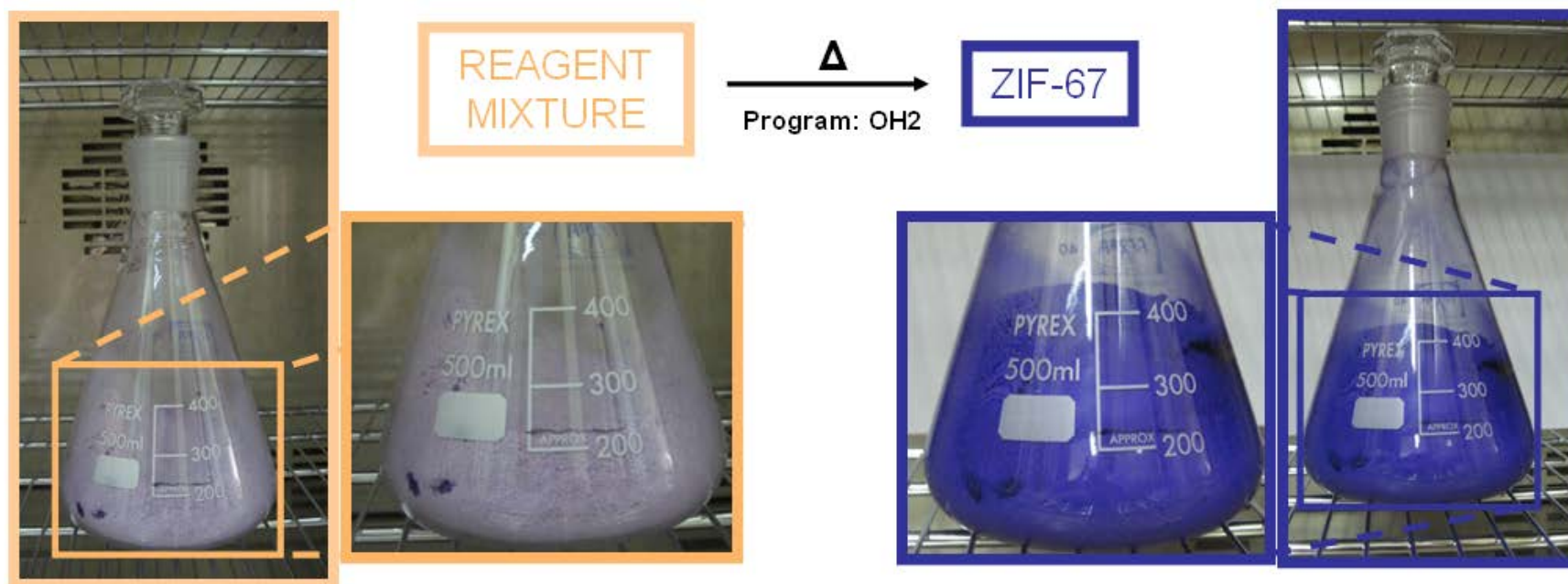


Figure S1.1. Scale up (200g) synthesis of ZIF-67 (ZIF67-OH2). Notice the volume and colour change.

S2. THERMOGRAVIMETRIC ANALYSIS AND FTIR SPECTRA

TGA measurements and FTIR spectra of representative samples are shown in Figures S2.1 and S2.2, respectively. The results of the thermogravimetric analyses and main FTIR bands gathered in Table S2.1.

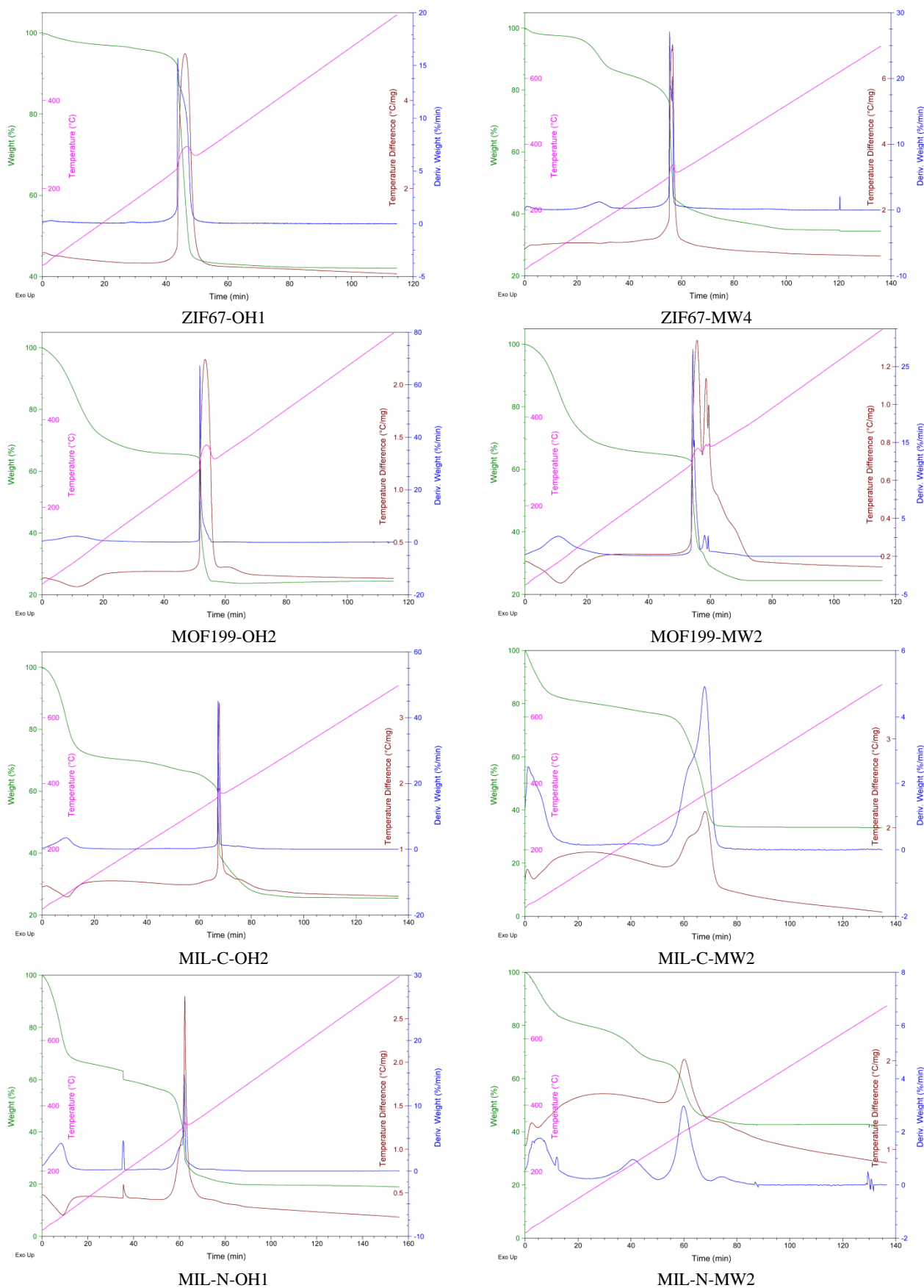


Figure S2.1. Thermogravimetric measurements performed upon representative samples.

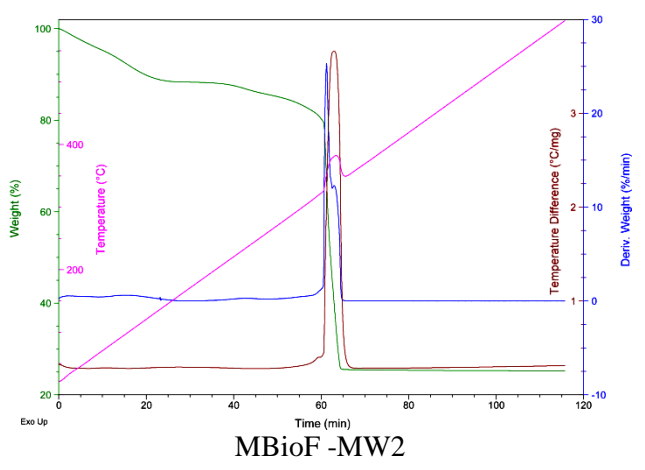
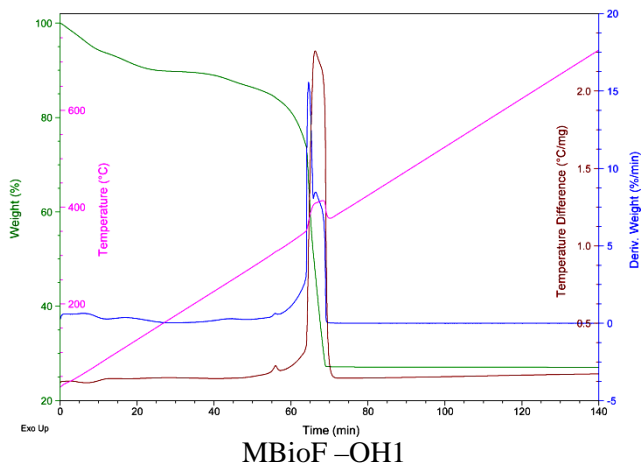


Figure S2.1 (cont.). Thermogravimetric measurements performed upon representative samples.

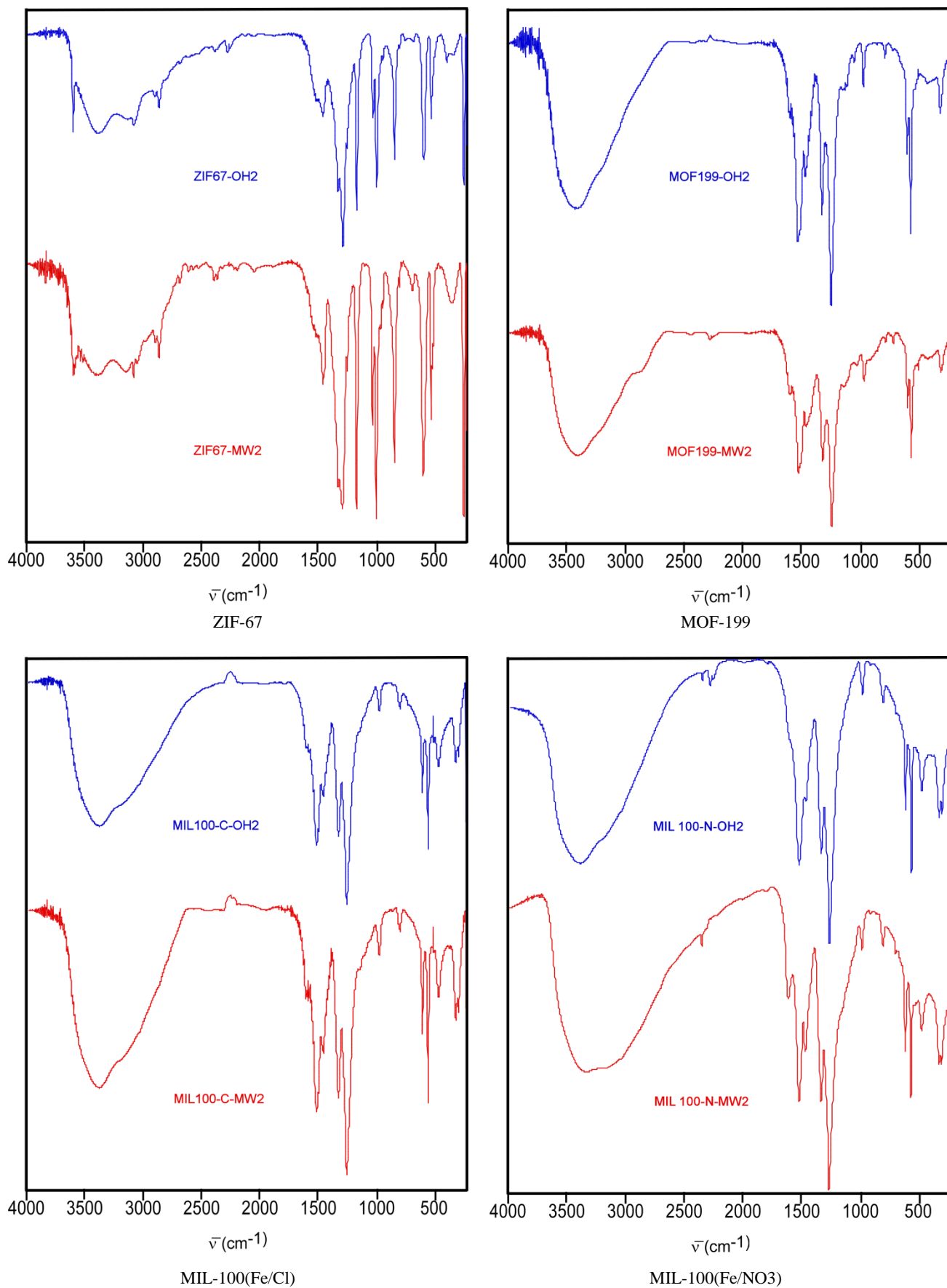


Figure S2.2. FTIR spectra performed upon representative samples.

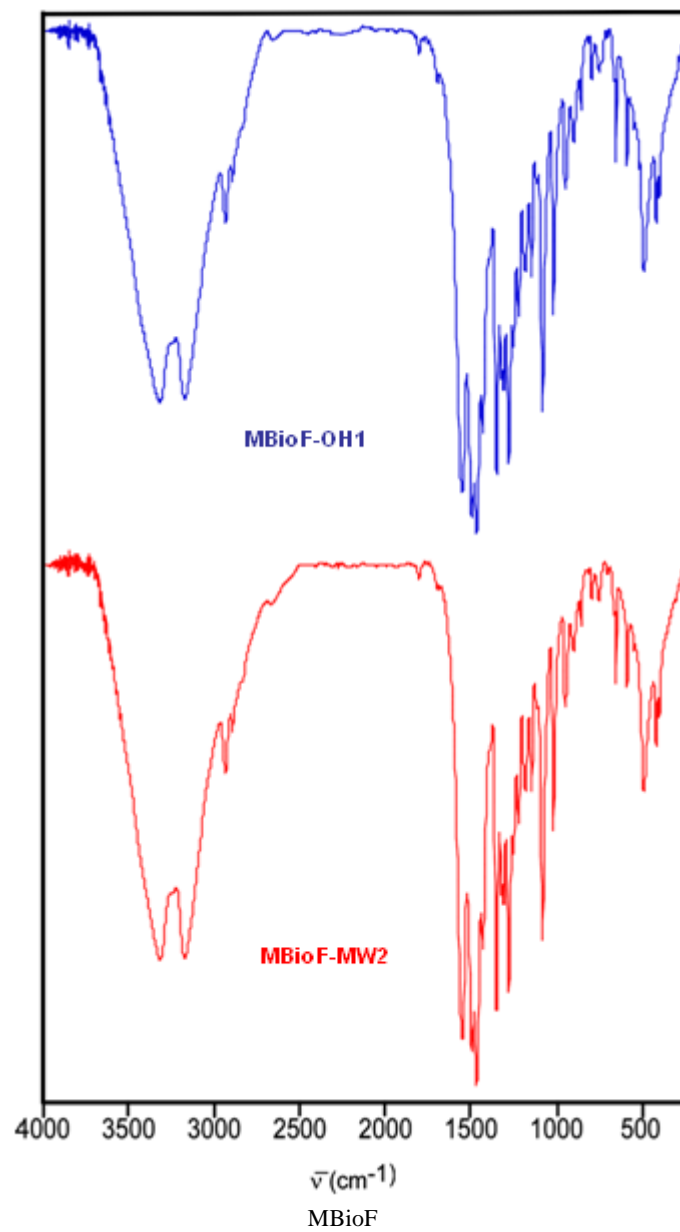


Figure S2.2 (cont.). FTIR spectra performed upon representative samples.

Table S2.1. Results of the thermogravimetric analyses and main FTIR bands for each sample.^a

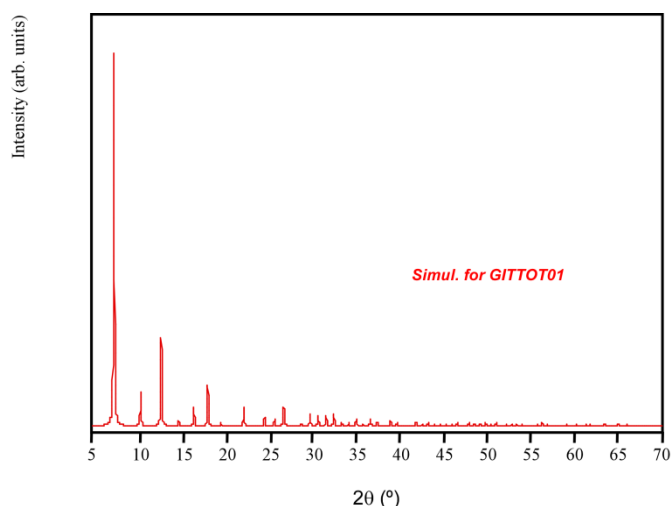
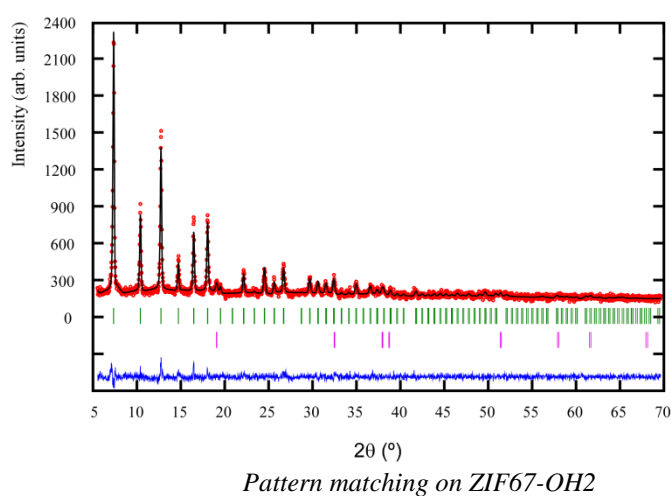
MOF	Formula	Sample	Residue of the thermogravimetry	Main FTIR bands (cm ⁻¹ , KBr pellets)
ZIF-67	[Co(mIm) ₂] _n	ZIF67-OH2	Residue: Co ₃ O ₄ Calcd.: 28.26% Found: 35.25%	3421 (m), 3130 (m), 2962 (w), 2924 (w), 1633 (sh), 1578 (m), 1507 (w), 1454 (s), 1414 (vs), 1383 (m), 1303 (s), 1172 (m), 1139 (s), 1087 (w), 992 (m), 950 (w), 835 (w), 750 (m), 692 (m), 683 (sh), 561 (w) 507 (sh), 425 (s).
	[Co(C ₄ H ₅ N ₂) ₂] _n	ZIF67-MW1	Residue: Co ₃ O ₄ Calcd.: 28.29% Found: 36.32%	3625 (m), 3444 (m), 3201 (m), 3132 (m), 3104 (sh), 2958 (w), 2923 (m), 2757 (w), 2472 (w), 2444 (w), 1580 (m), 1420 (vs), 1310 (vs), 1172(s), 1144 (vs), 994 (s), 755 (s), 694(m), 422 (vs).
MOF-199	[Cu ₃ (μ ₆ -BTC) ₂ (OH ₂) ₃] _n	MOF199-OH2	Residue: CuO Calcd.: 25.92% Found: 24.37%	3440 (s), 1710 (w), 1640 (s), 1580 (m), 1450 (s), 1370 (vs), 1270 (w), 1180 (w), 1110 (w), 940 (w), 870 (w), 760 (m), 720 (s), 670 (w), 590 (w), 490 (m).
	[Cu ₃ (μ ₆ -C ₉ H ₃ O ₆) ₂ (OH ₂) ₃] _n	MOF199-MW2	Residue: CuO Calcd.: 25.43% Found: 24.46%	3436 (s), 1710 (w), 1640 (s), 1580 (m), 1450 (s), 1374 (vs), 1270 (sh), 1110 (w), 940 (w), 870 (w), 760 (m), 730(s), 660 (w), 590 (w), 491 (w).
MIL-100 (Fe/Cl)	[Fe ₃ (μ ₃ -O)(μ ₆ -BTC) ₂ Cl(OH ₂) ₂] _n	MIL-C-OH2	Residue: Fe ₂ O ₃ Calcd.: 25.10% Found: 25.60%	3420 (s), 1628 (s), 1580(sh), 1450(s), 1380(vs), 1120 (w), 950 (w), 760 (m), 720 (s), 625 (m), 485 (m), 462 (m).
	[Fe ₃ (μ ₃ -O)(μ ₆ -C ₉ H ₃ O ₆) ₂ Cl(OH ₂) ₂] _n	MIL-C-MW2	Residue: Fe ₂ O ₃ Calcd.: 26.19% Found: 29.63%	3420 (s), 1716 (sh), 1633 (s), 1580 (m), 1450 (s), 1381 (vs), 1114 (w), 943 (w), 758 (m), 711 (s), 627 (m), 486 (m), 461 (m).
MIL-100 (Fe/NO ₃)	[Fe ₃ (μ ₃ -O)(μ ₆ -BTC) ₂ (NO ₃)(OH ₂) ₂] _n	MIL-N-OH2	Residue: Fe ₂ O ₃ Calcd.: 22.67% Found: 19.62%	3431 (s), 2421 (sh), 2357 (w), 1631 (s), 1576 (sh), 1553 (s), 1380 (vs), 1113 (w), 942 (w), 759 (m), 709 (s), 628 (m), 488 (m), 462 (m).
	[Fe ₃ (μ ₃ -O)(μ ₆ -C ₉ H ₃ O ₆) ₂ (NO ₃)(OH ₂) ₂] _n	MIL-N-MW4'	Residue: Fe ₂ O ₃ Calcd.: 27.48% Found: 25.72%	3379 (s), 1716 (w), 1621 (s), 1579 (m), 1442 (s), 1379 (vs), 1113 (w), 939 (w), 757 (m), 709 (s), 624 (w), 484 (m), 459 (m).
MBioF-12	[Co ₂ (μ ₃ -propionato) ₂ (μ-adeninato) ₂] _n	MOF-12-OH1	Residue: Co ₃ O ₄ Calcd.: 28.26% Found: 28.07%	3350(s), 3200(s), 2990(m), 2940(m), 1797(w), 1658 (vs), 1605(vs)□ 1578(vs),1542(s), 1464(s), 1439(s), 1425(s),1397(s), 1371(s), 1342(m), 1314(sh), 1304(m), 1271(m), 1242(m), 1210(s), 1149(m), 1082(m), 1033(w), 994(w), 953(w), 934(w), 895(w), 877(w), 798(m), 737(m), 712(m), 699(m), 667(m), 642(m), 574(m), 555(m)
	[Co ₂ (μ ₃ -C ₅ H ₅ N ₅) ₂ (μ-C ₃ H ₅ O ₂) ₂] _n	MOF-12-MW3	Residue: Co ₃ O ₄ Calcd.: 28.29% Found: 25.72%	3340(s), 3208(s), 2979(m), 2937(m), 1797(w), 1658 (vs), 1603(vs)□ 1578(vs),1542(s), 1464(s), 1439(s), 1425(s),1397(s), 1372(s), 1342(m), 1314(sh), 1306(m), 1269(m), 1242(m), 1207(s), 1149(m), 1079(m), 1032(w), 993(w), 950(w), 935(w), 896(w), 849(w), 799(m), 737(m), 712(m), 697(m), 643(m), 573(m), 554(m)

^a: calculated residue was obtained by assigning the mass value after the solvent removal to the formula of the activated MOF (i.e. calculated residue is obtained on the basis of the activated MOF formula and the mass after the removal of the solvent captured during the sample washing or adsorbed humidity. As the experimental mass percentage is different at this point, the calculated residue differs from one sample to another).

S3. X-RAY POWDER DIFFRACTION ANALYSIS

The X-ray powder diffraction (XRPD) patterns were collected on a Phillips X'PERT powder diffractometer with Cu-K α radiation ($\lambda = 1.5418 \text{ \AA}$) over the range $5 < 2\theta < 70$ with a step size of 0.02° and an acquisition time of 2.5 s per step at 20°C . Indexation of the diffraction profiles was made by means of the FULLPROF program (pattern-matching analysis)¹ on the basis of the space group and the cell parameters found in the *Cambridge Structural Database (CSD)* for the MOFs (elucidated by single crystal X-ray diffraction) and found in the *Inorganic Crystal Structure Database (ICSD)* for the corresponding metal hydroxide precursor. The calculated and observed diffraction patterns are shown in Figures S3.1-S3.3.

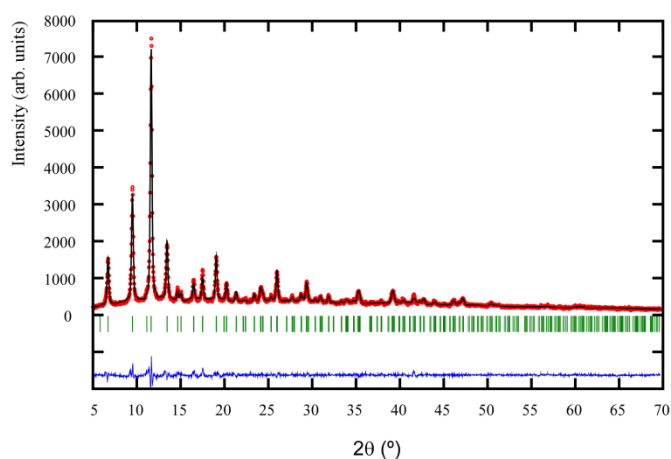
Reliability factors of the pattern-matching are calculated according to: $R_f = \frac{\sum (|I_{\text{obs}}|^{1/2} - |I_{\text{calc}}|^{1/2})}{\sum |I_{\text{obs}}|^{1/2}}$. $R_b = \frac{\sum |I_{\text{obs}} - I_{\text{calc}}|}{\sum I_{\text{obs}}}$. $R_p = \frac{\sum |y_{\text{obs}} - y_{\text{calc}}|}{\sum y_{\text{obs}}}$. $R_{wp} = \frac{[\sum \omega_i |y_{\text{obs}} - y_{\text{calc}}|^2 / \sum \omega_i (y_{\text{obs}})^2]^{1/2}}$.



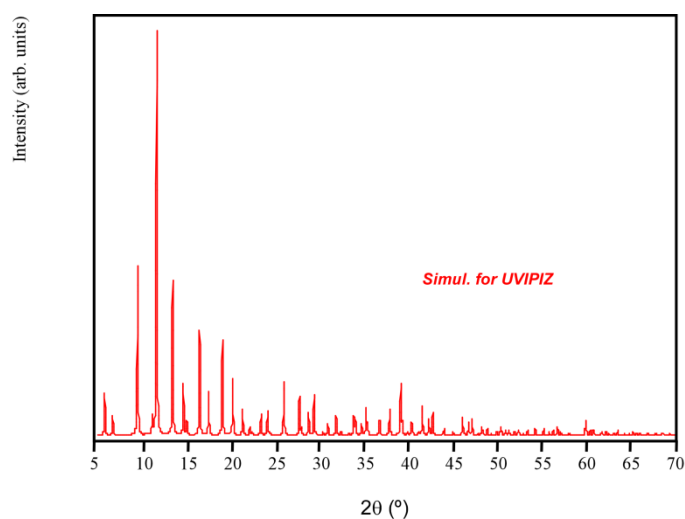
GITTOT01	
Crystal System	Cubic
Space group	I-43m
a (Å)	16.9589(3)
b (Å)	16.9589(3)
c (Å)	16.9589(3)
α (°)	90.00
β (°)	90.00
γ (°)	90.00
Fitting data	
2 θ range	5–70°
$\Delta 2\theta$	0.026°
R _f	5.30
R _b	1.97
R _p	6.01
R _{wp}	7.58
χ^2	1.23

Figure S3.1. Left-up: pattern-matching refinement on ZIF67-OH2 (green ticks: calculated reflections of GITTOT01 phase; pink ticks: calculated reflections of Co(OH)₂). Left-down: simulated PXRD pattern of GITTOT01. Right: Crystal structure data and pattern-matching refinement data.

¹ (a) Rodríguez-Carvajal, J. *FULLPROF, Program Rietveld for Pattern Matching Analysis of Powder Patterns*, Abstracts of the Satellite Meeting on Powder Diffraction of the XV Congress of the IUCr, Toulouse, Francia, **1990**, 127. (b) Rodríguez-Carvajal, J.: *FULLPROF 2000*, version 2.5d, Laboratoire Léon Brillouin (CEA-CNRS), Centre d'Études de Saclay, Gif sur Yvette Cedex, Francia, **2003**.

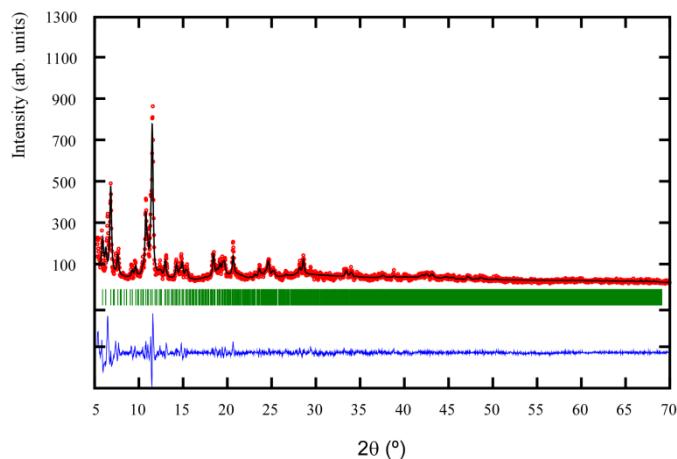


Pattern matching on MOF199-OH2

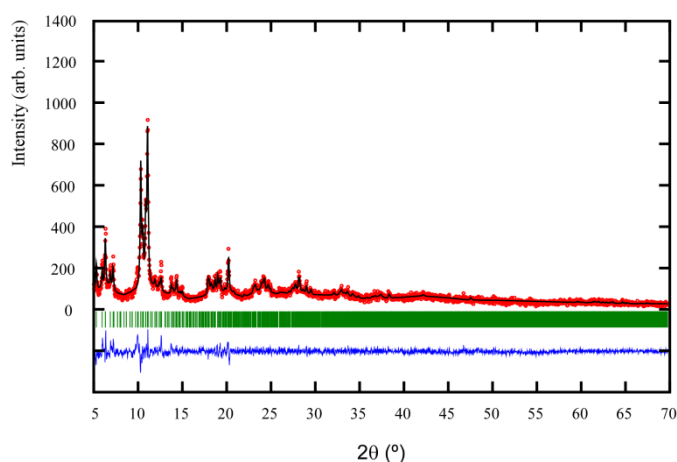


UVIPIZ	
Crystal System	Cubic
Space group	F m-3m
a (Å)	26.36053(7)
b (Å)	26.36053(7)
c (Å)	26.36053(7)
α (°)	90.00
β (°)	90.00
γ (°)	90.00
Fitting data	
2 θ range	5–70°
$\Delta 2\theta$	0.026°
Rf	1.60
Rb	0.76
Rp	5.23
Rwp	6.73
χ^2	1.92

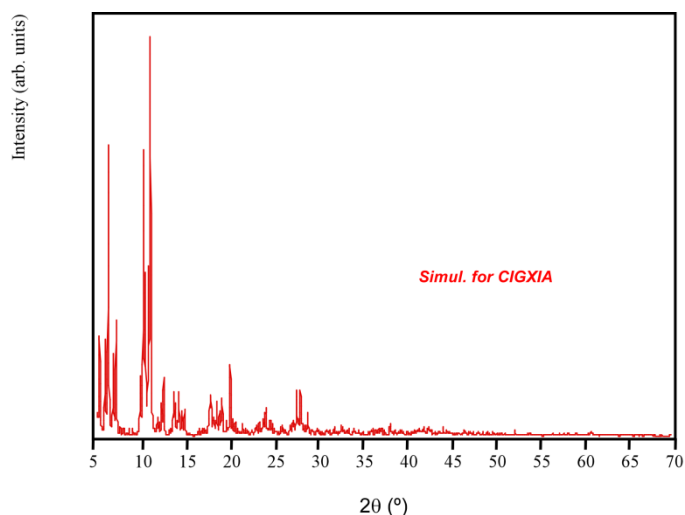
Figure S3.2. *Left-up:* pattern-matching refinement on MOF199-OH2 (green ticks: calculated reflections of UVIPIZ phase). *Left-down:* simulated PXRD pattern of UVIPIZ. *Right:* Crystal structure data and pattern-matching refinement data.



Pattern matching on MIL-C-OH2

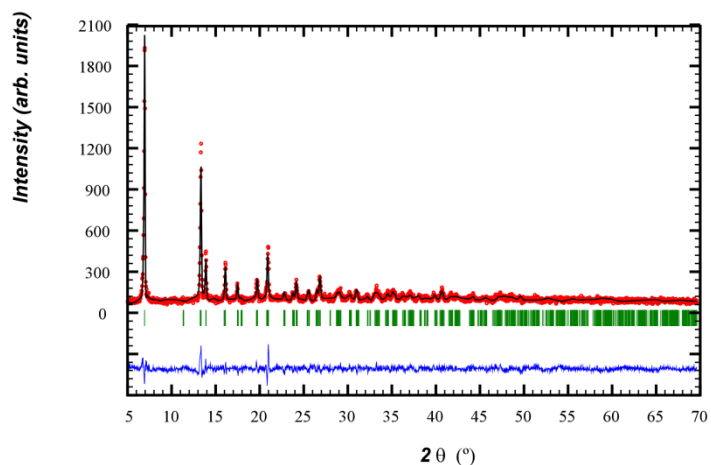


Pattern matching on MIL-N-OH2

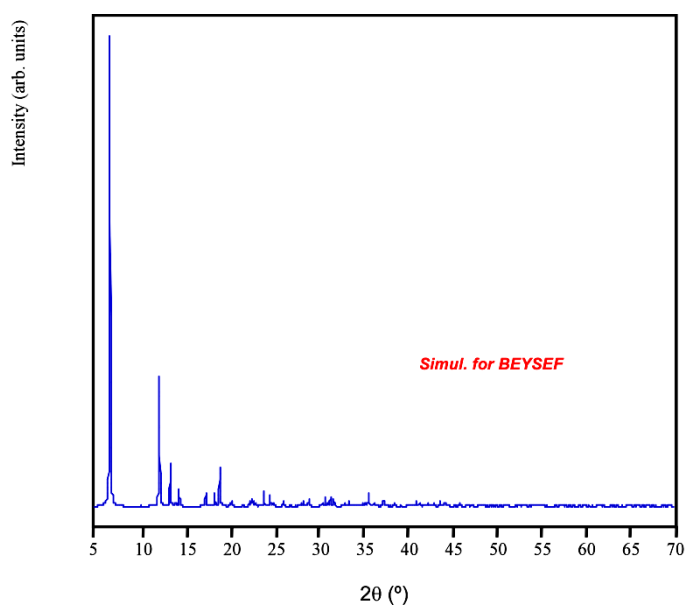


CIGXIA	
Crystal System	Cubic
Space group	F d-3m
a (Å)	73.340(1)
b (Å)	73.340(1)
c (Å)	73.340(1)
α (°)	90.00
β (°)	90.00
γ (°)	90.00
Fitting data for MIL-C-OH2	
2θ range	5–70°
Δ2θ	0.026°
Rf	11.1
Rb	2.81
Rp	19.2
Rwp	26.5
χ ²	3.44
Fitting data for MIL-N-OH2	
2θ range	5–70°
Δ2θ	0.026°
Rf	8.50
Rb	6.29
Rp	11.4
Rwp	15.8
χ ²	1.82

Figure S3.3. Left-up: pattern-matching refinement on MIL-C-OH2 and MIL-N-OH2 (green ticks: calculated reflections of CIGXIA phase). Left-down: simulated PXRD pattern of CIGXIA. Right: Crystal structure data and pattern-matching refinement data.



Pattern matching on MBioF-OH1



BEYSEF	
Crystal System	Tetragonal
Space group	I – 4 ₁ /a
a (Å)	17.243(3)
b (Å)	17.243(3)
c (Å)	20.157(6)
α (°)	90.00
β (°)	90.00
γ (°)	90.00
Fitting data	
2θ range	5–70°
Δ2θ	0.026°
Rf	2.91
Rb	1.83
Rp	9.92
Rwp	12.7
χ ²	1.99

Figure S3.4. *Left-up:* pattern-matching refinement on MBioF (green ticks: calculated reflections of BEYSEF phase). *Left-down:* simulated PXRD pattern of BEYSEF. *Right:* Crystal structure data and pattern-matching refinement data.

S4. EFFECT OF THE HEATING RATES AND SOURCE ON SAMPLE CRYSTALLINITY

In order to assess the effect of the solvent-free synthesis conditions on the materials properties, samples were prepared either varying the oven heating rates and microwave irradiation times. According to the PXRD patterns of Figures S4.1–S4.4 the lowering of the heating rate promotes a substantial increase in crystallinity of the samples. Regarding to the samples prepared by microwave heating, non meaningful differences are observed among the diffraction patterns of different irradiation times, but all them are less crystalline than those samples prepared under conventional heating. It deserves to note that in each compound all patterns are plotted at the same count scale. Figures S4.5-4.9 show a comparison of the SEM images for samples prepared under oven heating and microwave irradiation. The appearance of all samples is that of a polycrystalline one, with submicrometric crystallite sizes.

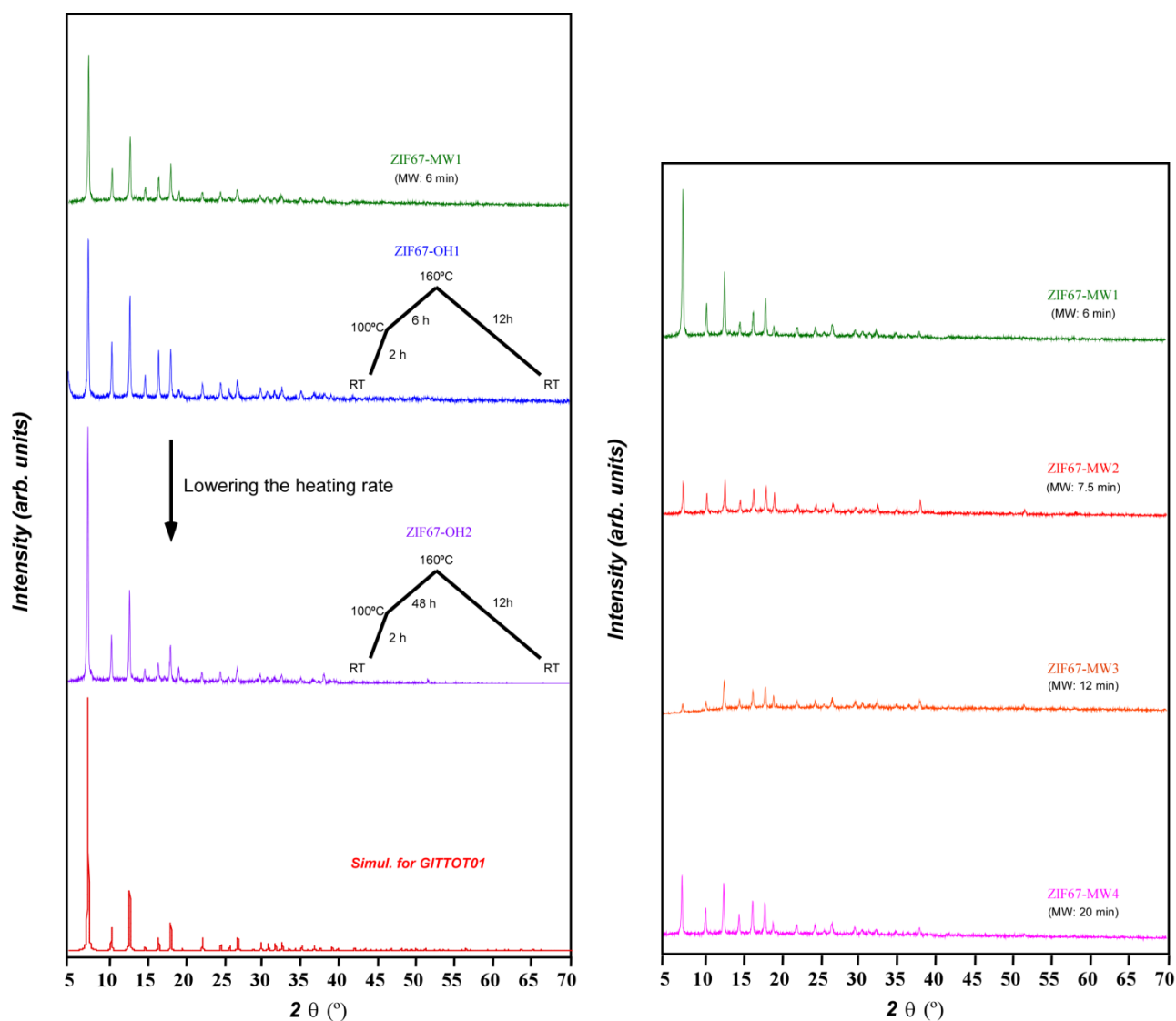


Figure S4.1. A comparison among the PXRD patterns of ZIF-67 samples prepared at different oven heating rates and microwave irradiation times.

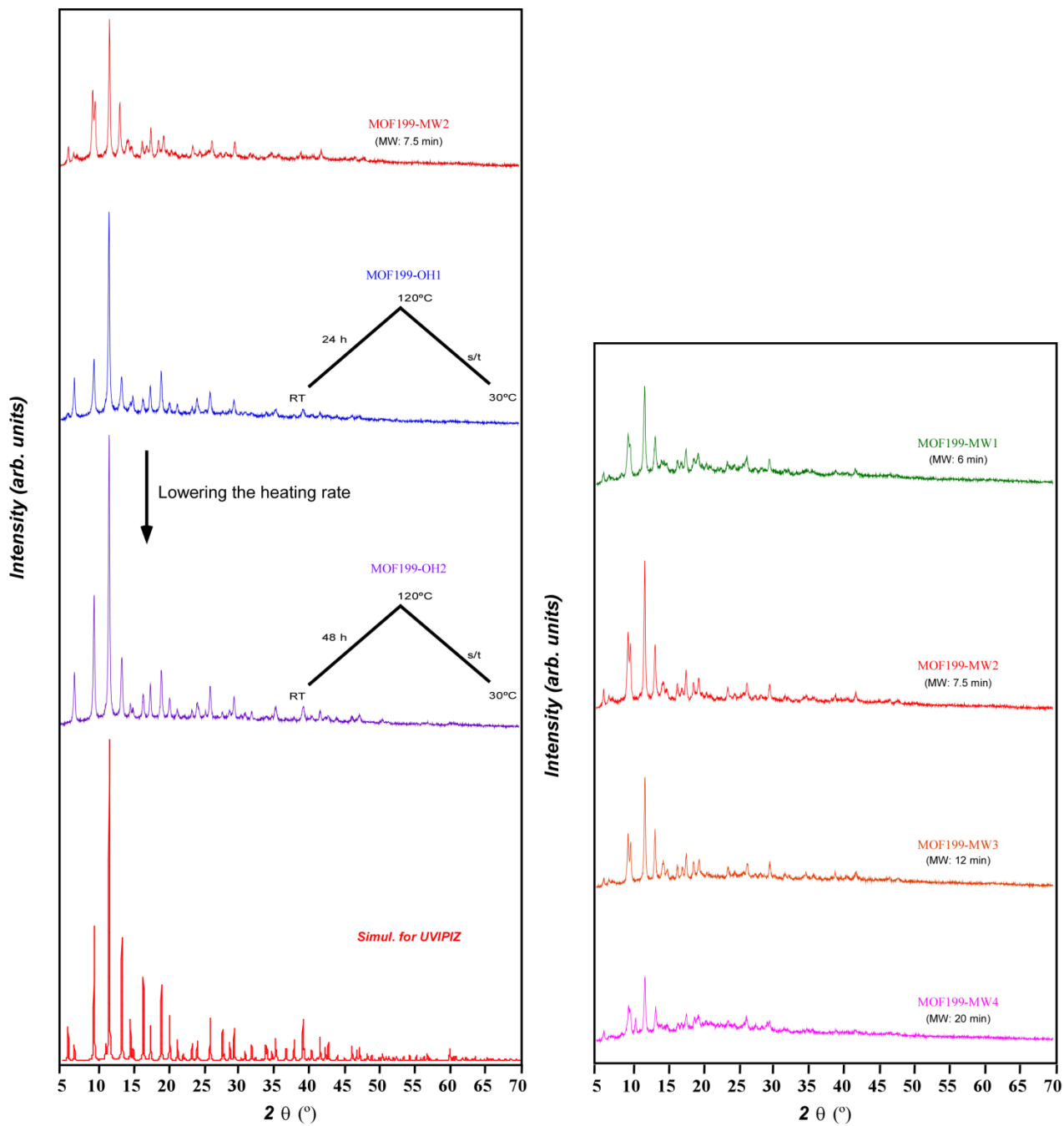


Figure S4.2. A comparison among the PXRD patterns of MOF-199 samples prepared at different oven heating rates and microwave irradiation times.

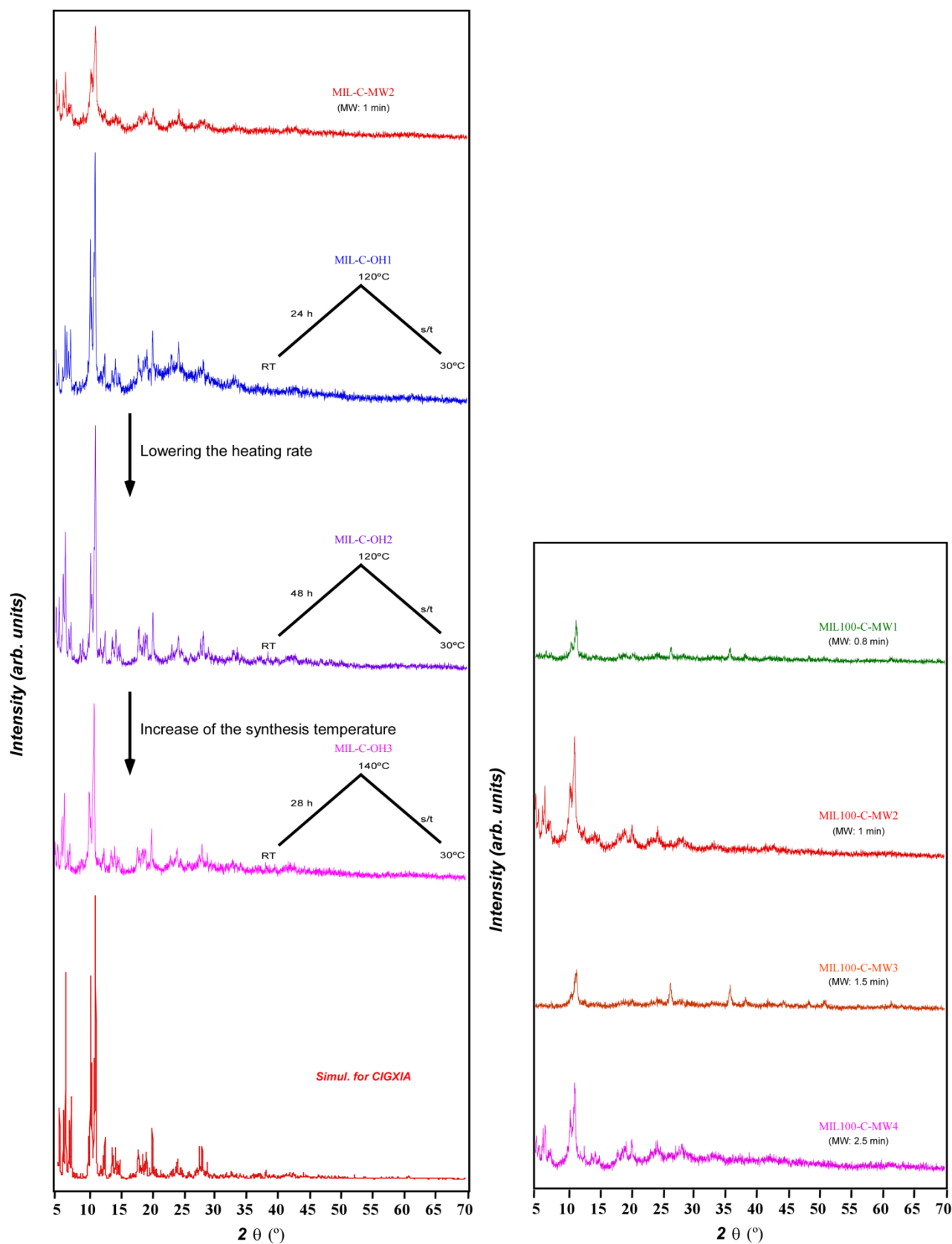


Figure S4.3. A comparison among the PXRD patterns of MIL-100(Fe/Cl) samples prepared at different oven heating rates and microwave irradiation times.

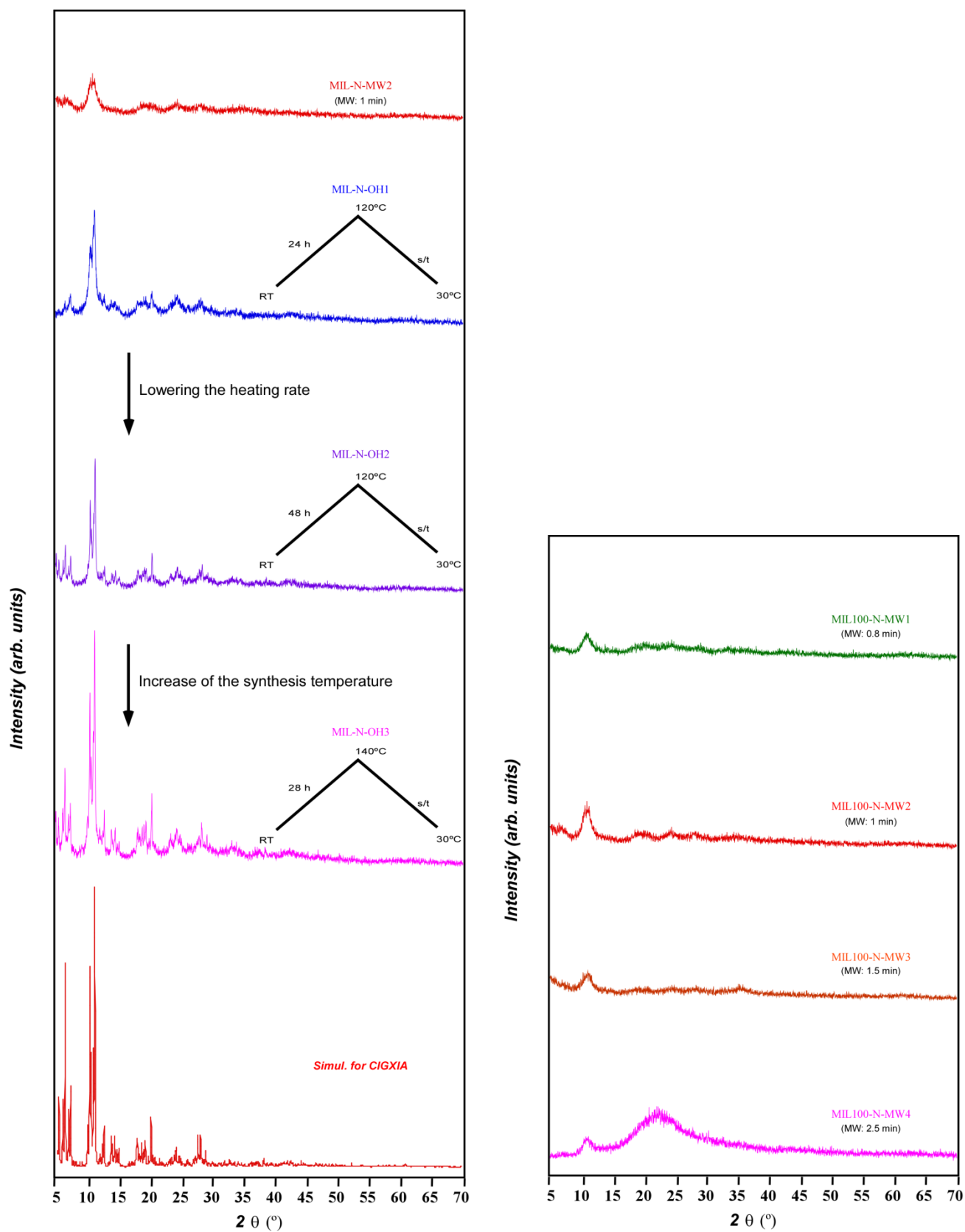


Figure S4.4. A comparison among the PXRD patterns of MIL-100(Fe/NO₃) samples prepared at different oven heating rates and microwave irradiation times.

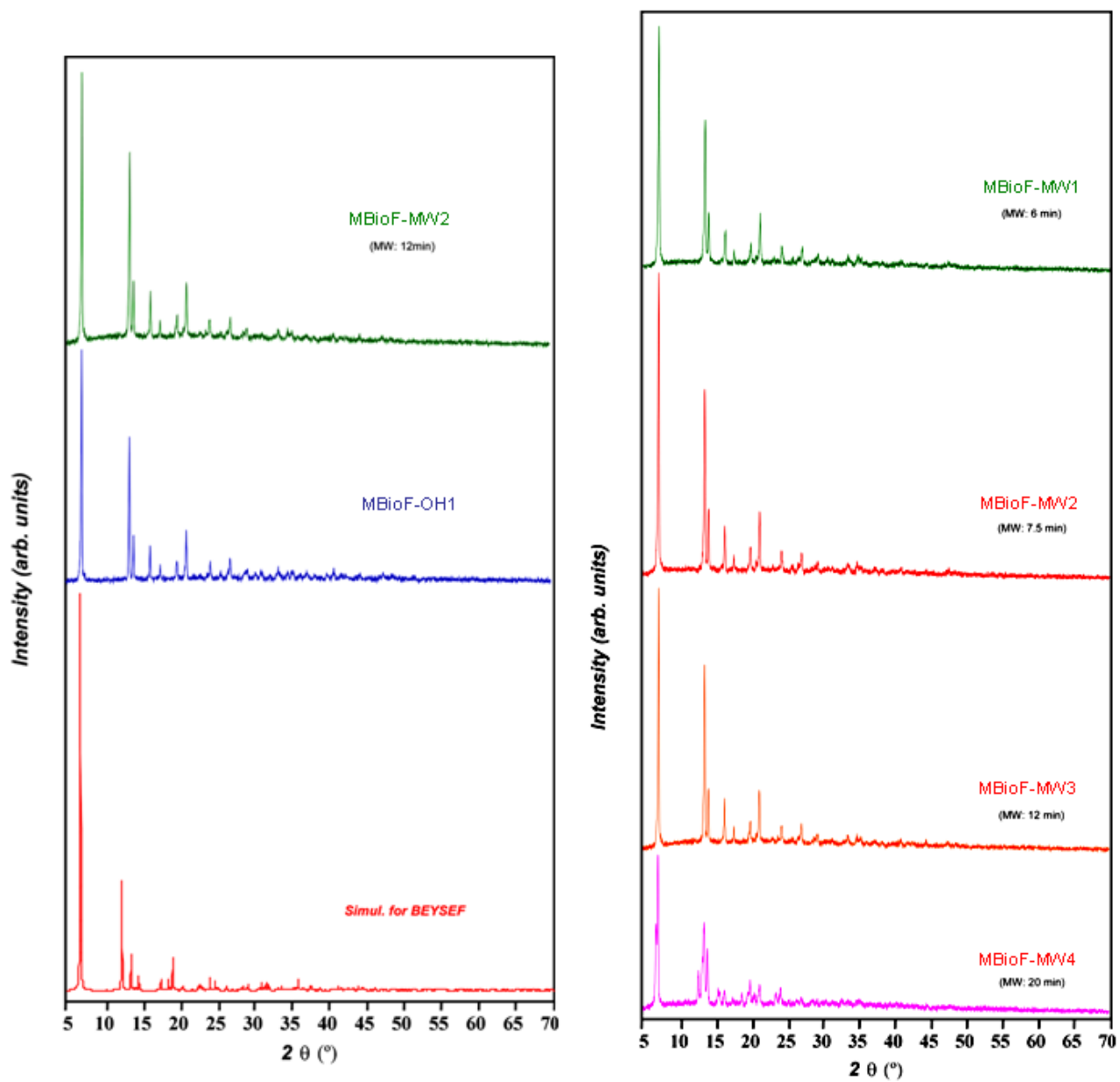
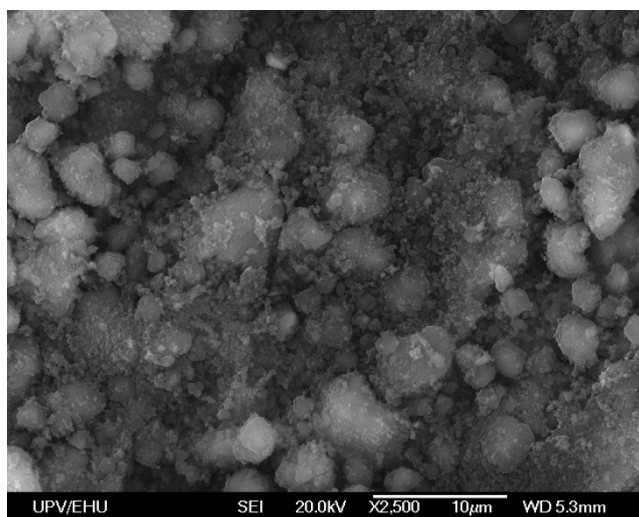
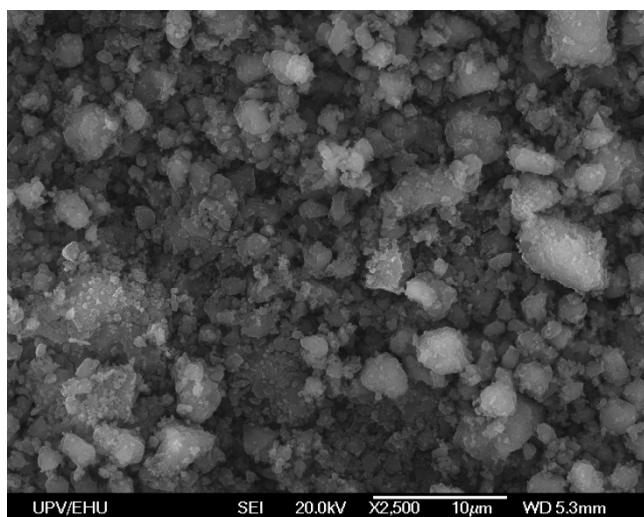


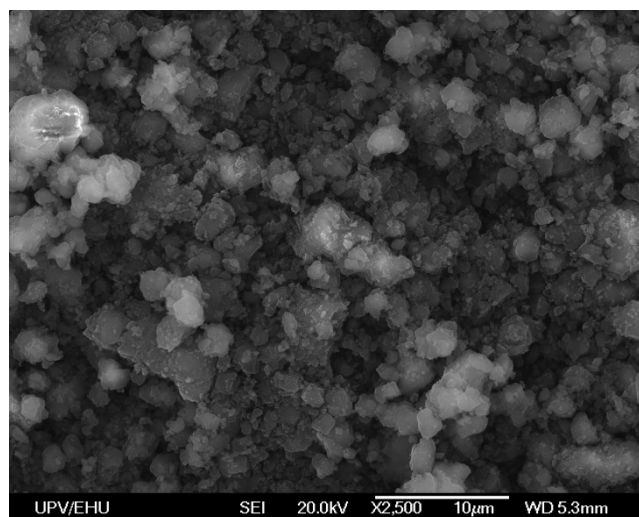
Figure S4.5. A comparison among the PXR patterns of MBioF samples prepared at different oven heating rates and microwave irradiation times.



ZIF67-OH2

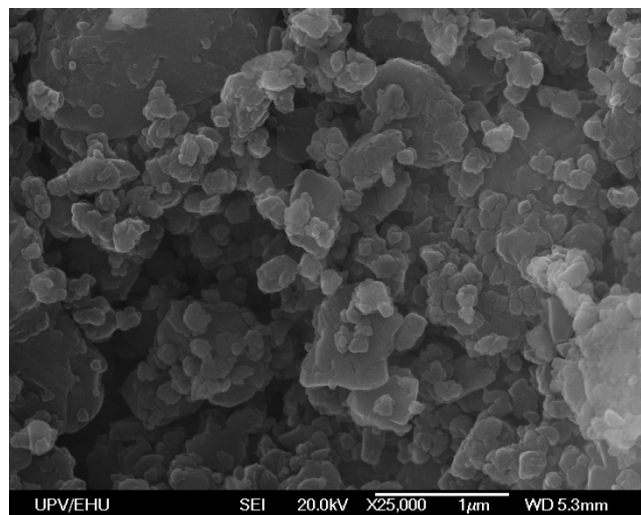


ZIF67-MW1

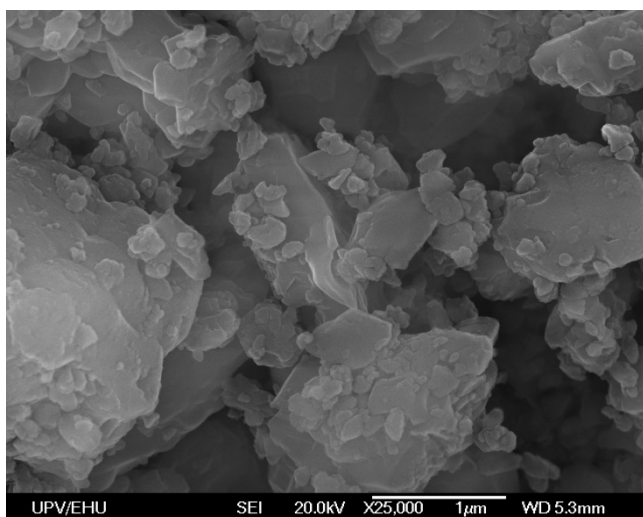


ZIF67-MW2

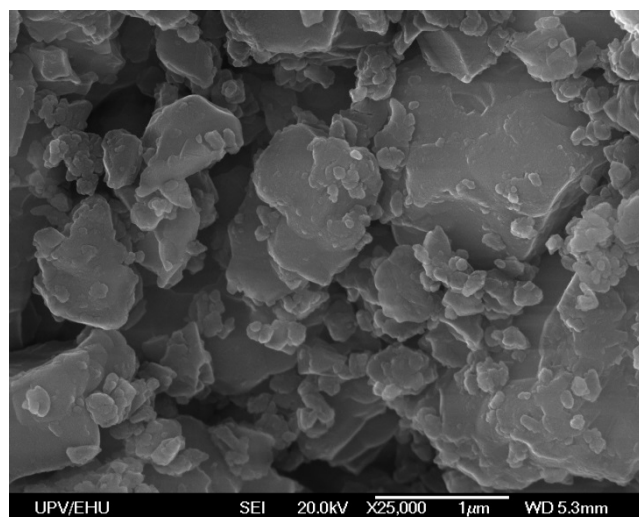
Figure S4.5. SEM images at 2.5 kX of ZIF-67 samples prepared by oven heating and microwave irradiation.



ZIF67-OH2

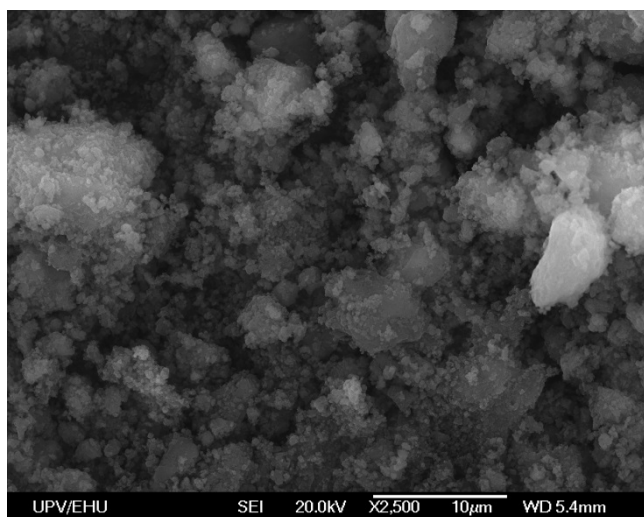


ZIF67-MW1

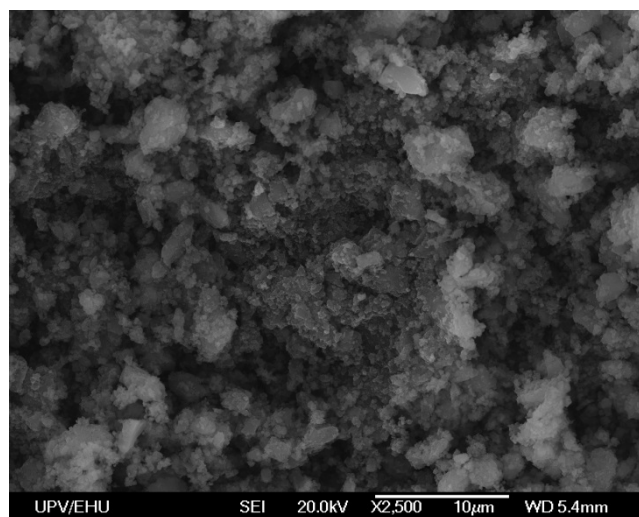


ZIF67-MW2

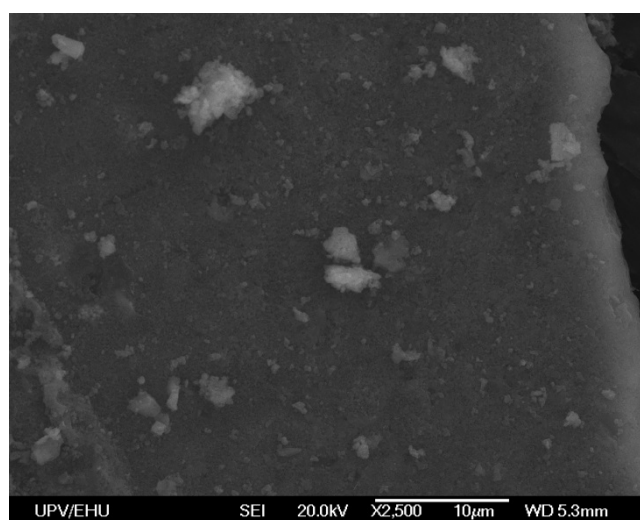
Figure S4.6. SEM images at 25 kX of ZIF-67 samples prepared by oven heating and microwave irradiation.



MOF199-OH1

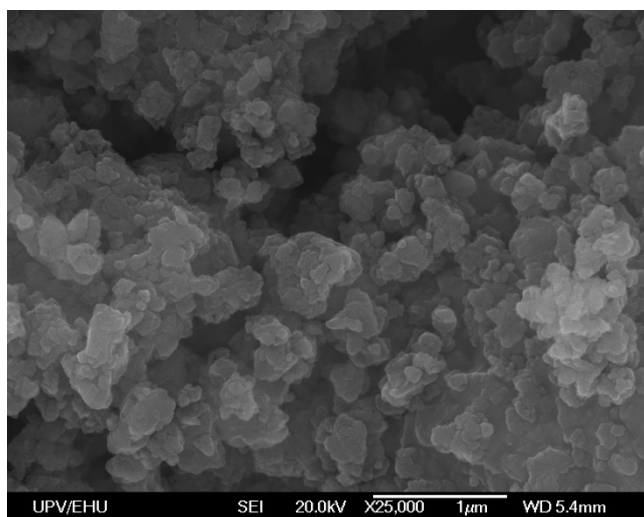


MOF199-OH2

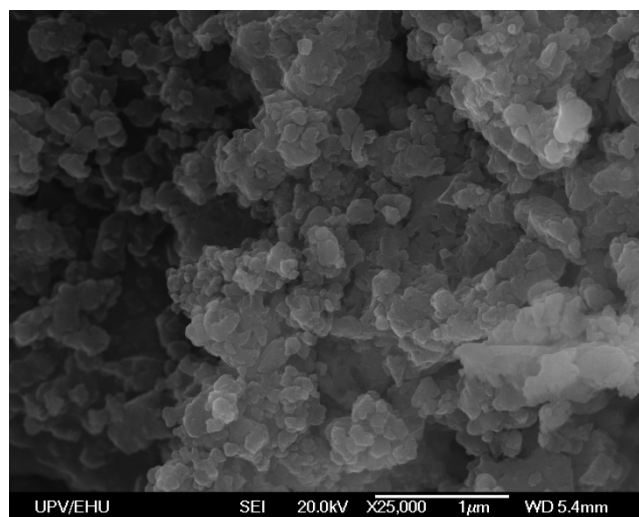


MOF199-MW2

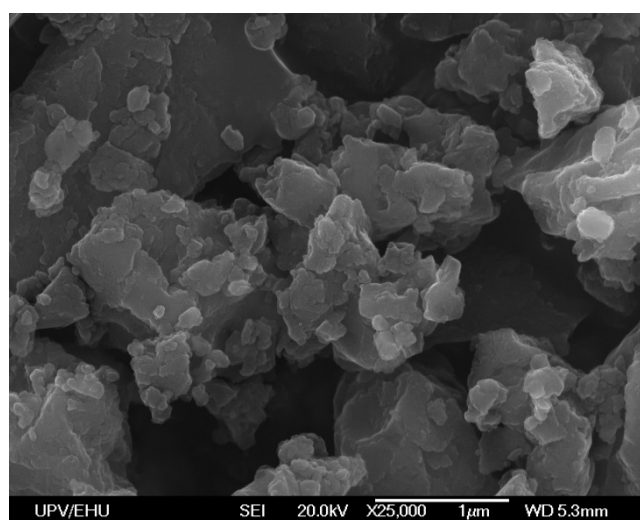
Figure S4.7. SEM images at 2.5 kX of MOF-199 samples prepared by oven heating and microwave irradiation.



MOF199-OH1



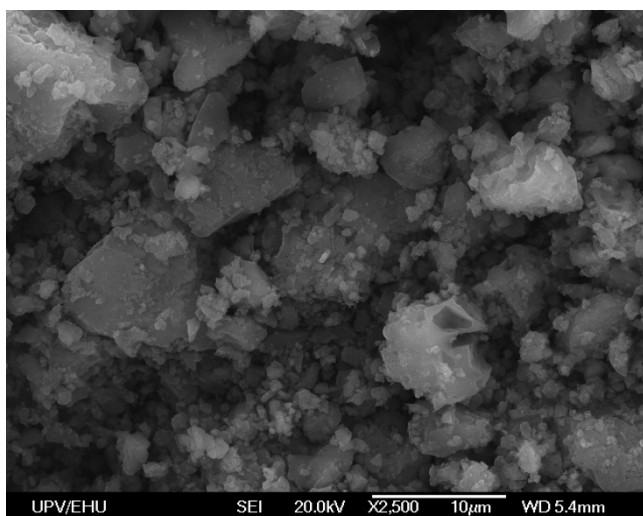
MOF199-OH2



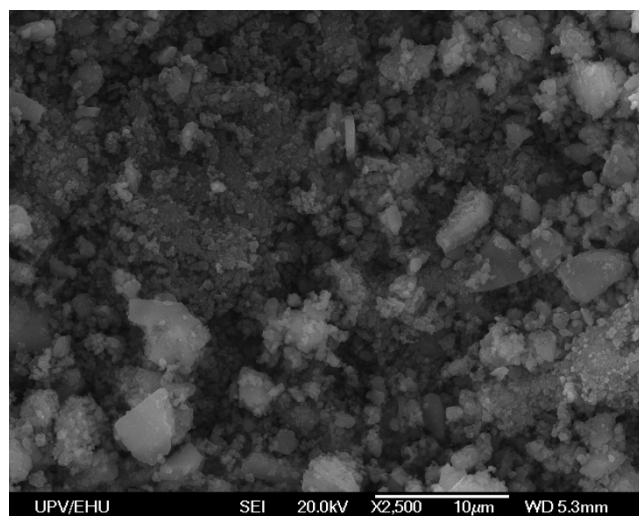
MOF199-MW2

Figure S4.8. SEM images at 25 kX of MOF-199 samples prepared by oven heating and microwave irradiation.

2.5 kX

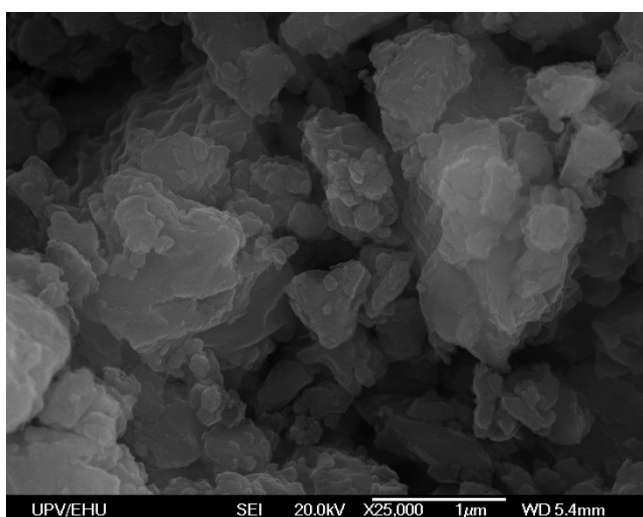


MIL-CI-OH2

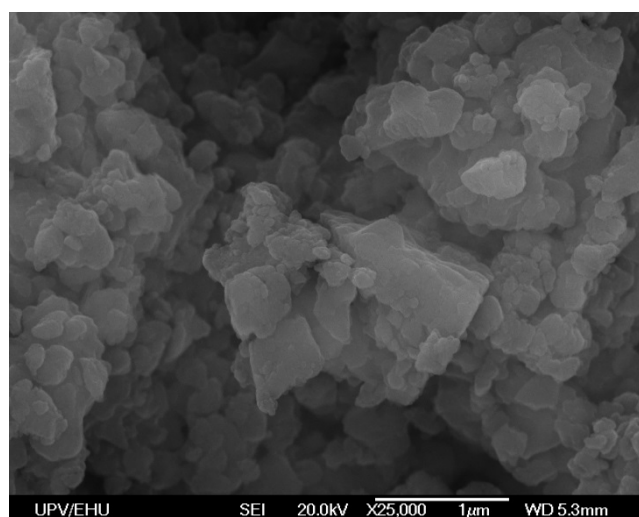


MIL-CI-MW2

25 kX



MIL-CI-OH2



MIL-CI-MW2

Figure S4.9. SEM images at 2.5 and 25 kX of MIL-100(Fe/Cl) samples prepared by oven heating and microwave irradiation.

S5. N₂ ADSORPTION EXPERIMENTS

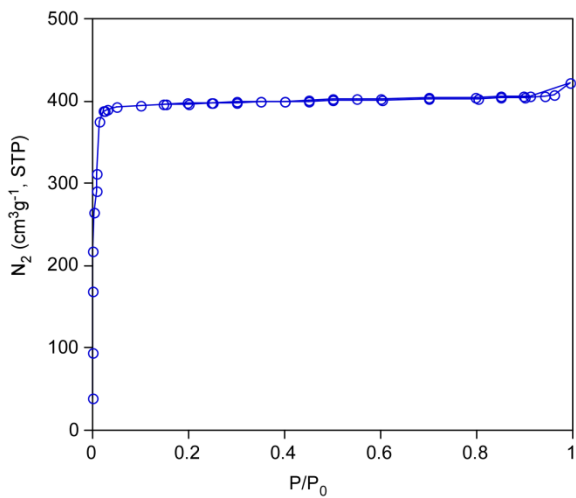
The permanent porosity was studied by means of the measurements of N₂ adsorption isotherms at 77 K (Figure S5.1 and S5.2) using a *Micromeritics* ASAP 2010 analyser. All samples were dried under vacuum at 140°C during six hours to eliminate solvent guest molecules prior to measurements. It deserves to note that the crystallinity of the outgassed samples was retained as confirmed by XRPD measurements.

The surface area values were obtained by the fittings of the adsorption data to Braunauer-Emmett-Teller (BET) equation. In order to choose the pressure range appropriate and to avoid ambiguity when reporting the BET surface area of MOFs, we used the three consistency criteria proposed by Walton and Snurr:² (1) The pressure range selected should have values of V(P₀ - P) increasing with P/P₀. (2) The points used to calculate the BET surface area must be linear with an upward slope. (3) The line they form must have a positive y-intercept. This procedure is commonly applied for determining the BET surface area values of high/ultrahigh MOFs.³

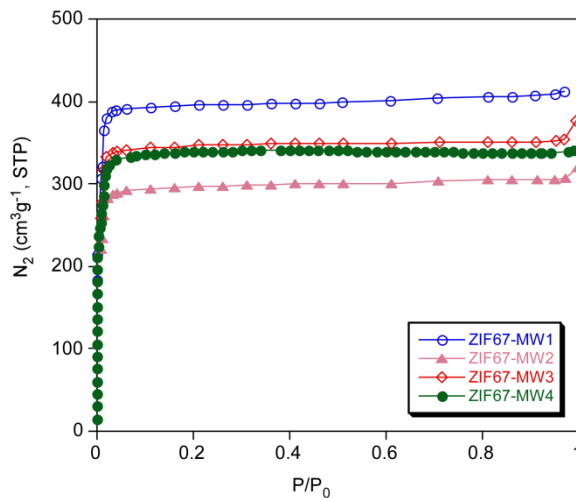
The V(P₀ - P) vs P/P₀ plots used to define the pressure range according to the first consistency criteria are showed in Figure S5.3 and S5.4. BET fitting data is gathered in Table 5.1.

² K. S. Walton, R. Q. Snurr, *J. Am. Chem. Soc.* **2007**, *127*, 8552.

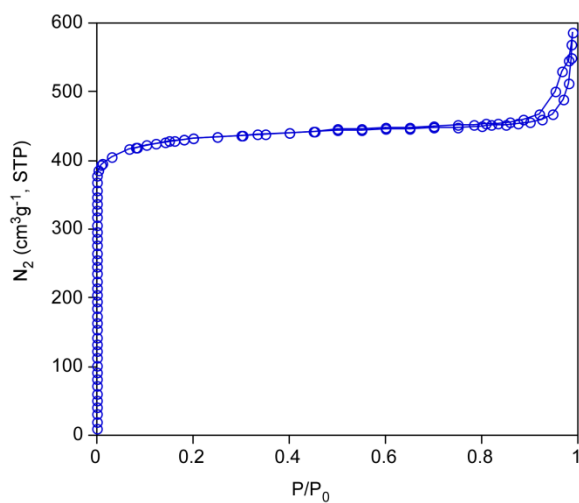
³ (a) O. K. Farha, A. O. Yazaydin, I. Eryazici, C. D. Malliakas, B. G. Hauser, M. G. Kanatzidis, S. T. Nguyen, R. Q. Snurr, J. T. Hupp, *Nat. Chem.* **2010**, *2*, 944. (b) H. Furukawa, N. Ko, Y. B. Go, N. Aratani, S. B. Choi, E. Choi, A. O. Yazaydin, R. Q. Snurr, M. O'Keeffe, J. Kim, O. M. Yaghi, *Science* **2010**, *329*, 424. (c) O. K. Farha, I. Eryazici, N. C. Jeong, B. G. Hauser, C. E. Wilmer, A. A. Sarjeant, R. Q. Snurr, S. T. Nguyen, A. O. Yazaydin and J. T. Hupp, *J. Am. Chem. Soc.* **2012**, *134*, 15016.



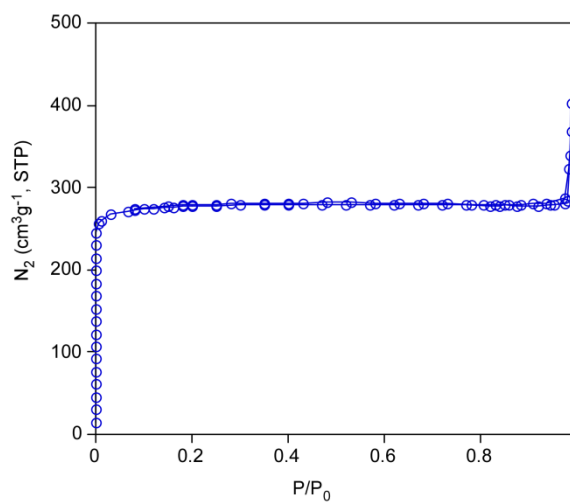
ZIF67-OH1



ZIF67-MW1 / ZIF67-MW2 / ZIF67-MW3 / ZIF67-MW4



MOF199-OH2



MOF199-MW2

Figure S5.1. Nitrogen adsorption isotherms at 77 K for ZIF-67 and MOF-199 compounds.

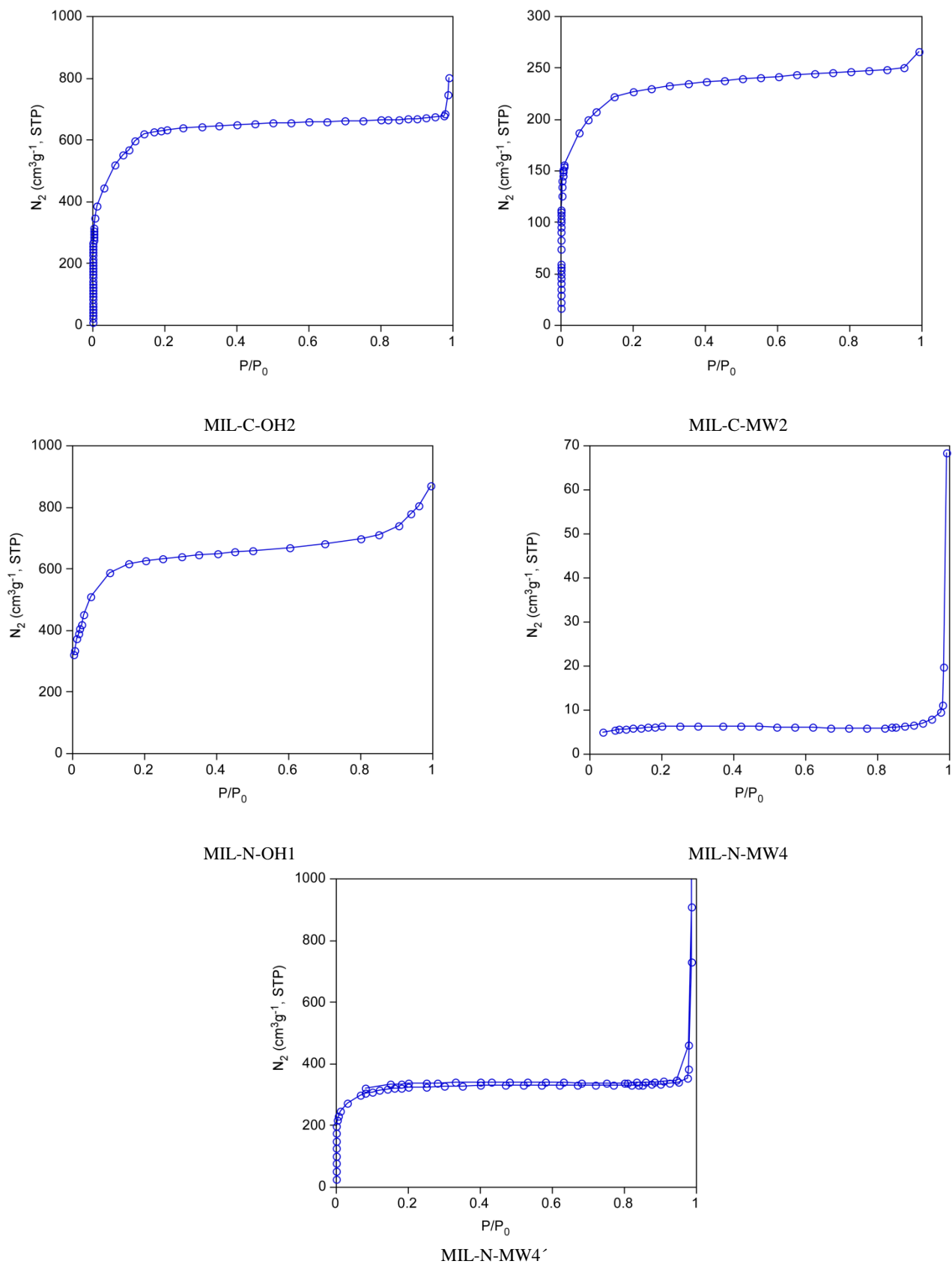
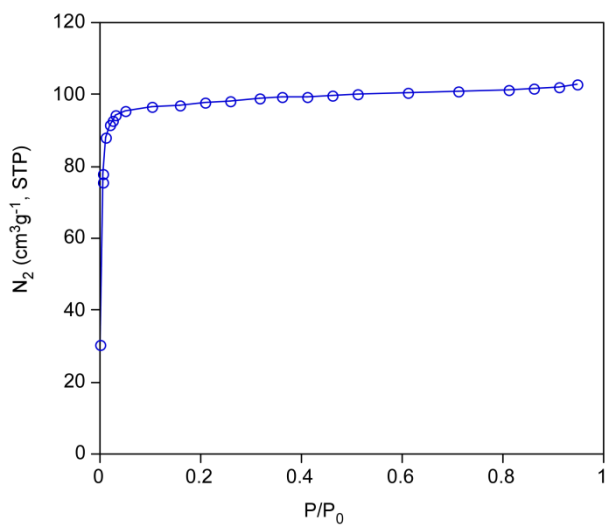
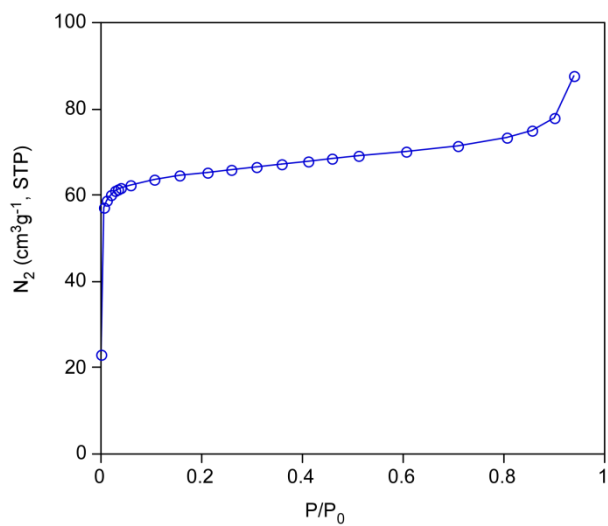


Figure S5.2. Nitrogen adsorption isotherms at 77 K for MIL-100(Fe/Cl) and MIL-100(Fe/NO₃) compounds.

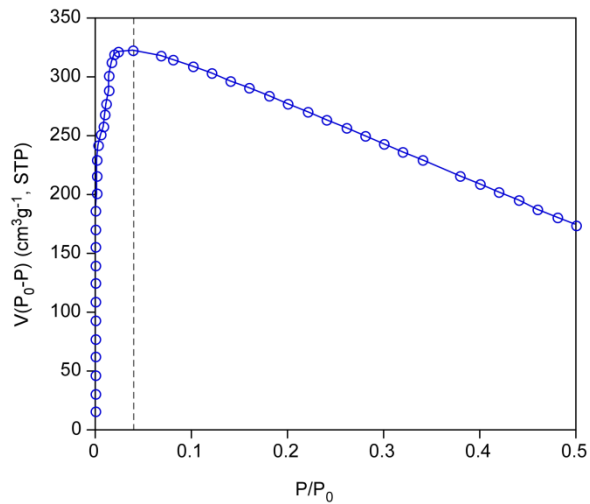
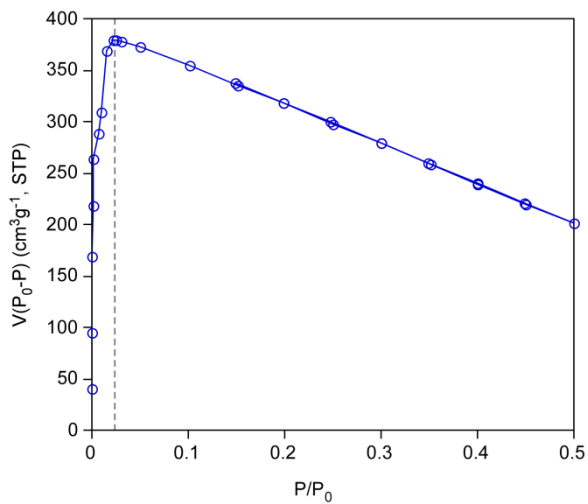


MBioF-OH1



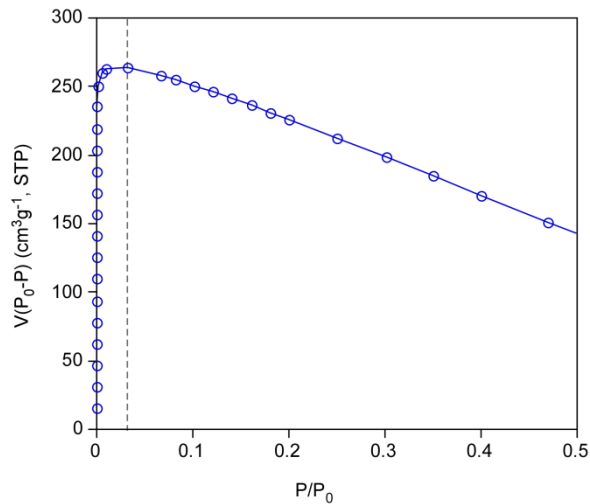
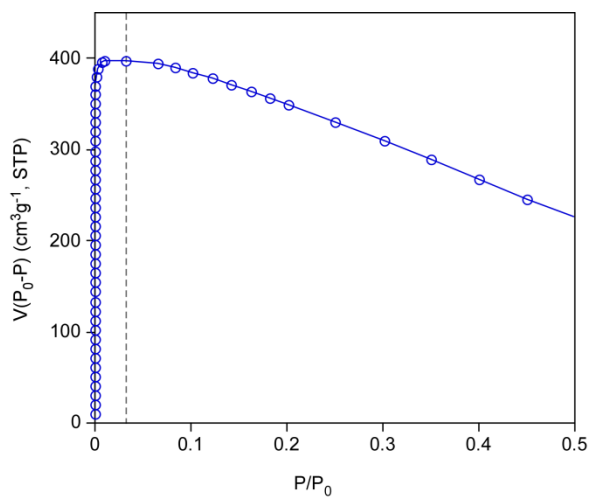
MBioF-MW2

Figure S5.3. Nitrogen adsorption isotherms at 77 K for MBioF-12 compounds.



ZIF67-OH1

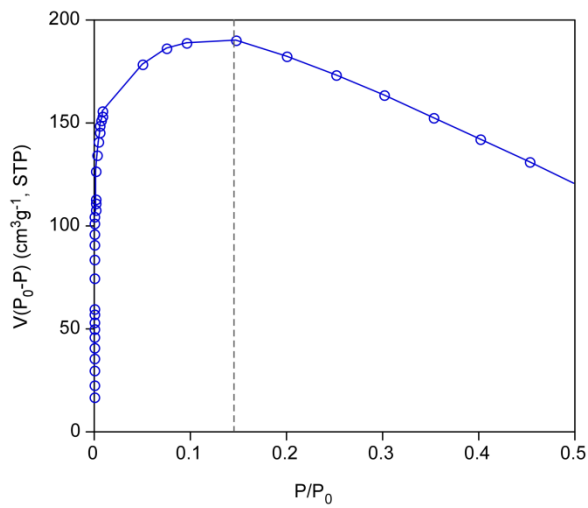
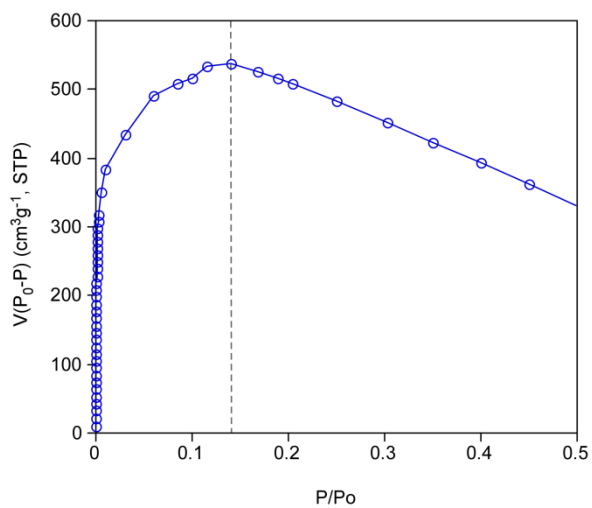
ZIF67-MW4



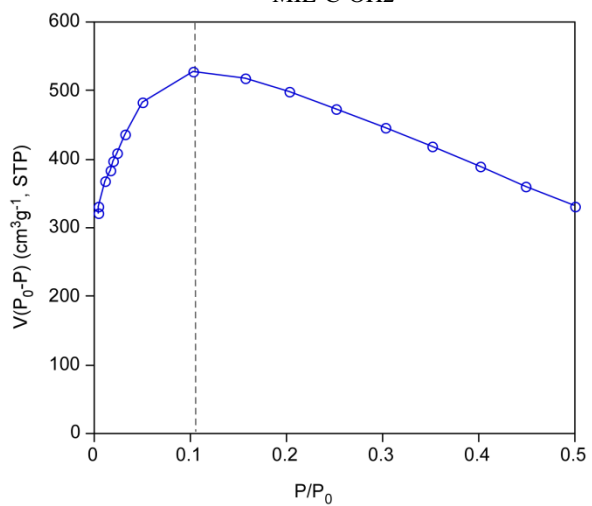
MOF199-OH2

MOF199-MW2

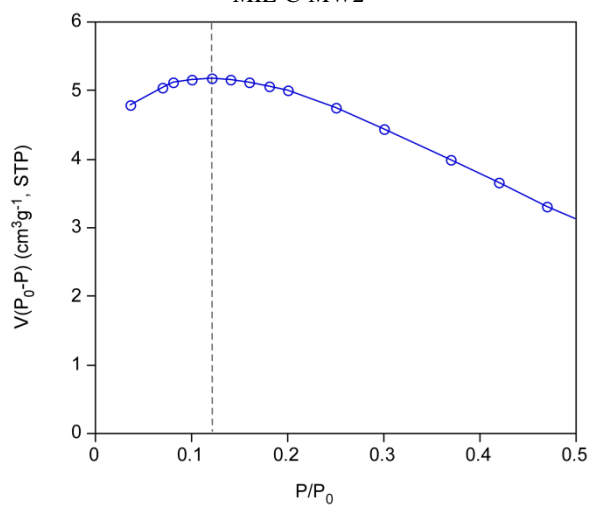
Figure S5.4. Consistency plot $[V(P_0 - P)$ vs. $P/P_0]$ for experimental N_2 isotherms.



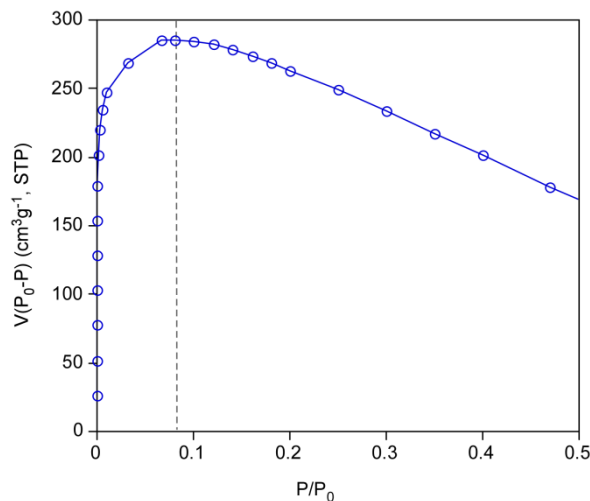
MIL-C-OH2



MIL-C-MW2



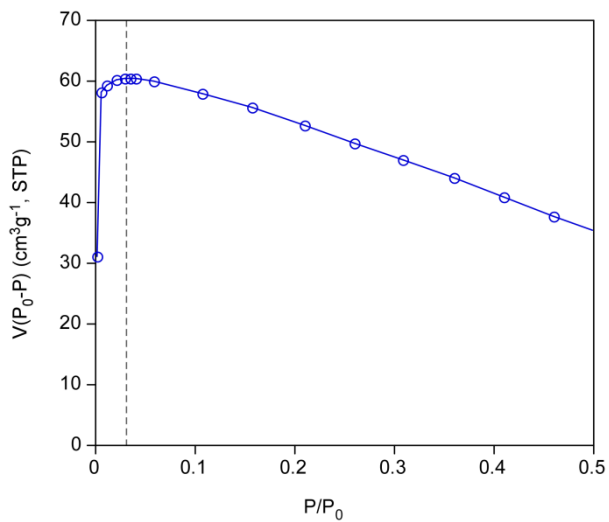
MIL-N-OH1



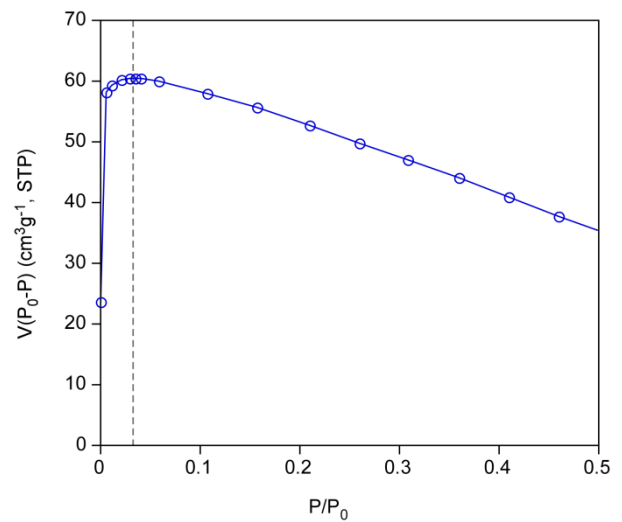
MIL-N-MW4

MIL-N-MW4'

Figure S5.5. Consistency plot [$V(P_0 - P)$ vs. P/P_0] for experimental N_2 isotherms.



MBioF-OH1



MBioF-MW2

Figure S5.6. Consistency plot [$V(P_0 - P)$ vs. P/P_0] for experimental N_2 isotherms.

Table 5.1. BET fitting data.

Sample	Pressure range	Slope	Intercept	R ²	<i>c</i>	Area (m ² /g)
ZIF67-OH1	0.0150–0.0396	$1.94 \cdot 10^{-3}$	$4.263 \cdot 10^{-6}$	0.9980	361.0	1851
ZIF67-MW1	0.0097–0.0313	$2.41 \cdot 10^{-3}$	$6.70 \cdot 10^{-6}$	0.9963	361.0	1799
ZIF67-MW2	0.0090–0.0329	$3.20 \cdot 10^{-3}$	$1.12 \cdot 10^{-5}$	0.9970	311.2	1355
ZIF67-MW3	0.0087–0.0340	$2.79 \cdot 10^{-3}$	$7.06 \cdot 10^{-6}$	0.9950	368.6	1555
ZIF67-MW4	0.0082–0.0140	$2.87 \cdot 10^{-3}$	$9.919 \cdot 10^{-6}$	0.9996	313.5	1512
MOF199-OH2	0.0008–0.0319	$2.54 \cdot 10^{-3}$	$1.02 \cdot 10^{-7}$	0.9999	$24.8 \cdot 10^3$	1713
MOF199-MW2	0.0002–0.0316	$3.85 \cdot 10^{-3}$	$2.21 \cdot 10^{-7}$	0.9999	$17.4 \cdot 10^3$	1130
MIL-C-OH2	0.0604–0.1409	$1.73 \cdot 10^{-3}$	$2.05 \cdot 10^{-5}$	0.9992	85.1	2492
MIL-C-MW2	0.0497–0.1478	$5.11 \cdot 10^{-3}$	$2.32 \cdot 10^{-5}$	0.9999	221.7	849
MIL-N-OH1	0.0198–0.1029	$1.74 \cdot 10^{-3}$	$1.66 \cdot 10^{-5}$	0.9998	105.6	2486
MIL-N-MW4	0.0689–0.1203	$1.86 \cdot 10^{-1}$	$7.30 \cdot 10^{-4}$	0.9999	256.1	23
MIL-N-MW4'	0.0052–0.0802	$3.49 \cdot 10^{-3}$	$6.37 \cdot 10^{-6}$	0.9997	549.5	1245
MBioF-OH1	0.0062–0.0252	$1.05 \cdot 10^{-2}$	$1.34 \cdot 10^{-5}$	0.9996	784.1	415
MBioF-MW2	0.0118–0.0402	$1.68 \cdot 10^{-2}$	$4.23 \cdot 10^{-6}$	0.9999	3962.8	260

S6. COMPARATIVE BETWEEN SYNTHESIS ROUTE AND SURFACE AREA

Table 6.1. A comparative between the synthesis route and achieved BET surface area value.

Synthesis Type	Solvent	Reagents	Areas (m ² /g)	Reference
ZIF-67				
Solvent-free	--	Co(OH) ₂	1851	<i>This work</i>
MW-solvent-free	--	Co(OH) ₂	1799	<i>This work</i>
Steam assisted	water	Co(OAc) ₂ , HmIm	1319	⁴
Stirring	water	Cu(NO ₃) ₂ , HmIm, TEA	868	⁵
Stirring	water	Cu(NO ₃) ₂ , HmIm	316	⁶
MOF-199				
MW-Solvothermal	DMF	Cu(NO ₃) ₂ , H ₃ BTC	1944	⁷
Solvent-free	--	Cu(OAc) ₂ , H ₃ BTC	1713	<i>This work</i>
Solvothermal	DMF	Cu(OAc) ₂ , H ₃ BTC	1507	⁸
MW-solvent-free	--	Cu(OAc) ₂ , H ₃ BTC	1130	<i>This work</i>
Sonochemical	DMF	Cu(NO ₃) ₂ , H ₃ BTC	1100	⁹
Solvothermal	water/ethanol	Cu(NO ₃) ₂ , H ₃ BTC	692	¹⁰
Solvothermal	ethanol	Cu(NO ₃) ₂ , H ₃ BTC	1656	¹¹
Electrochemical	methanol	Cu ⁰ , H ₃ BTC	1820	¹²
MIL100-(Fe/X); X: F⁻, Cl⁻, NO₃⁻.				
Solvent-free	--	FeX ₃ , H ₃ BTC	2492	<i>This work</i>
Solvothermal	water	Fe ⁰ , H ₃ BTC, HF, HNO ₃	2320	¹³
MW-solvent-free	--	FeCl ₃ , H ₃ BTC	849	<i>This work</i>
MW-Solvothermal	water	FeCl ₃ , H ₃ BTC, HF, HNO ₃	1474	¹⁴
Spray drying	water	FeCl ₃ , H ₃ BTC	1000	¹⁵
Solvothermal	water/ethanol	FeCl ₃ , H ₃ BTC	860-1350	¹⁶
<i>Solvothermal</i>	<i>water</i>	<i>FeCl₃, H₃BTC</i>	<i>1136</i>	¹⁷

⁴ Q. Shi, Z. Chen, Z. Song, J. Li, J. Dong, *Angew. Chem. Int. Edit.*, **2011**, 50, 672.

⁵ A. F. Gross, E. Sherman, J. J. Vajo, *Dalton Trans.*, **2012**, 41, 5458

⁶ N. Mntungwa, V. S. R. R. Pullabhotla, N. Revaprasadu, *Mater. Lett.*, **2012**, 82, 220.

⁷ A. G. Wong-Foy, A. J. Matzger, O. M. Yaghi, *J. Am. Chem. Soc.*, **2006**, 128, 3494.

⁸ J. L. C. Rowsell, O. M. Yaghi, *J. Am. Chem. Soc.*, **2006**, 128, 1304.

⁹ Z.-Q. Li, L.-G. Qiu, T. Xu, Y. Wu, W. Wang, Z.-Y. Wu, X. Jiang., *Mater. Lett.*, **2009**, 63, 78.

¹⁰ S. S.-Y. Chui, S. M.-F. Lo, J. P. H. Charmant, A. G. Orpen, I. D. Williams, *Science*, **1999**, 283, 1148.

¹¹ N. A. Khan, S. H. Jung, *Micropor. Mesopor. Mater.*, **2009**, 119, 331.

¹² U. Mueller, M. Schubert, F. Teich, H. Puetter, K. Schierle-Arndt, J. Pastré, *J. Mater. Chem.*, **2006**, 16, 626.

¹³ J. W. Yoon, Y.-K. Seo, Y. K. Hwang, J.-S. Chang, H. Leclerc, S. Wuttke, P. Bazin, A. Vimont, M. Daturi, E. Bloch, P. L. Llewellyn, C. Serre, P. Horcajada, J.-M. Grenche, A. E. Rodrigues, G. Férey. *Angew. Chem. Int. Edit.*, **2010**, 49, 5949.

¹⁴ J.-D. Xiao, L.-G. Qiu, X. Jiang, Y.-J. Zhu, S. Ye, X. Jiang, *Carbon*, **2013**, 59, 372.

¹⁵ A. Garcia Marquez, P. Horcajada, D. Grosso, G. Férey, C. Serre, C. Sanchez, C. Boissiere, *Chem. Commun*, **2013**, 49, 3848.

¹⁶ A. García Márquez, A. Demessence, A. E. Platero-Prats, D. Heurtaux, P. Horcajada, C. Serre, J.-S. Chang, G. Férey, V. A. De la Peña-O'Shea, C. Boissière, D. Grosso, C. Sanchez, *Eur. J. Inorg. Chem.* **2012**, 5165.

¹⁷ T. B. Čelič, M. Rangus, K. Lázár, V. Kaučič, N. Z Logar. *Angew. Chem. Int. Edit.* **2012**, 51, 12490.